Volume 7
Issue 2
December 2018

ISSN - 1857 - 839X

SJCE

SCIENTIFIC JOURNAL OF CIVIL ENGINEERING

SS CYRIL AND METHODIUS UNIVERSITY
FACULTY OF CIVIL ENGINERING

ISSN 1857-839X

EDITORIAL - Preface to Volume 7 Issue 2 of the Scientific Journal of Civil Engineering (SJCE)

Todorka Samardzioska EDITOR – IN - CHIEF

Dear Readers,

Dear Readers,
Scientific Journal of Civil Engineering (SJCE) was established in December 2012. It is published bi-annually and is available online at the web site of the Faculty of Civil Engineering in Skopje (www.gf.ukim.edu.mk).

This Journal welcomes original works within the field of civil engineering, which includes: all the types of engineering structures and materials, water engineering, geo-technics, highway and railroad engineering, survey and geo-spatial engineering, buildings and environmental protection, construction management and many others. The Journal focuses on analysis, experimental work, theory, practice and computational studies in the fields.

The international editorial board encourages all researchers, practitioners and members of the academic community to submit papers and contribute for the development and maintenance of the quality of the SJCE journal.

As an editor of the Scientific Journal of Civil Engineering, it is my pleasure to introduce the Second Issue of Volume 7.

This issue of our Journal is entirely devoted to topics of geotechnics and geodesy. This summer, Skopje was welcoming the XVI Danube-European Conference on Geotechnical Engineering (DECGE). The conference was held under the auspices of the International Society of Soil Mechanics and Geotechnical Engineering (ISSMGE), with the support of International Tunnelling and Underground Space Association, while the Faculty of Civil Engineering in Skopje was one of the domestic co-organizers. The first five papers in this issue were originally presented at the XVI Danube-European Conference on Geotechnical Engineering in June 2018 in Skopje, and they have been updated herein. They are devoted to numerical and experimental analysis of soils and foundations. The last two papers are in the field of application of surveying methods in seismic active regions.

To all of our readers, friends and colleagues

Have a prosperous New Year and
Merry Christmas!

May the next year be better, more successful, healthier and happier!

Sincerely Yours,

Prof. Dr. Sc. Todorka Samardzioska

December, 2018

SJCE
SCIENTIFIC JOURNAL OF CIVIL ENGINEERING

Impressum

FOUNDER AND PUBLISHER

Faculty of Civil Engineering - Skopje Partizanski odredi 24, 1000 Skopje

EDITORIAL OFFICE

Faculty of Civil Engineering - Skopje Partizanski odredi 24, 1000 Skopje Rep. of Macedonia tel. +389 2 3116 066; fax. +389 2 3118 834 email: prodekan.nauka@gf.ukim.edu.mk

EDITOR IN CHIEF

Prof. dr sc. **Todorka Samardzioska**

University Ss. Cyril and Methodius Faculty of Civil Engineering -Skopje Partizanski odredi 24, 1000 Skopje Republic of MACEDONIA
email: samardzioska@gf.ukim.edu.mk

ISSN: 1857-839X

ORDERING INFO

SJCE is published semiannually. All articles published in the journal have been reviewed.

Edition: 100 copies

SUBSCRIPTIONS

Price of a single copy: for Macedonia (500 den); for abroad (10 EUR + shipping cost).

BANKING DETAILS (MACEDONIA)

Narodna banka na RM

Account number: 160010421978815

Prihodno konto 723219

Programa 41

BANKING DETAILS (INTERNATIONAL)

Corespond bank details:

Deutsche Bundesbank Zentrale

Address:Wilhelm Epstein strasse 14 Frankfurt am Main, Germany

SWIFT BIC: MARK DE FF

Bank details:

National Bank of the Republic of Macedonia

Address: Kompleks banki bb 1000 Skopje Macedonia

SWIFT BIC:NBRM MK 2X

IBAN: MK 07 1007 0100 0036 254

Name: Gradezen fakultet Skopje

CONTENTS

Become a student of the Faculty of Civil Engineering and a part of the impetus that creates and build the world! Step in the world of the successful people, because even the longest roads start with the first step. You will spend a part of your youth with us, and the youth is expensive to be misspent in vain. Your choice is an exceptional profession, for people who do believe in themselves, profession that requires prompt and courageous decisions. This profession will provide you with great privileges: your actions will remain an eternal record in the space and in the time being.

- STRUCTURAL ENGINEERING
- HYDRO-TECHNICAL ENGINEERING
- ROADS AND RAILWAYS ENGINEERING
- GEODESY
- GEOTECHNICAL ENGINEERING

LT978.

SS CYRIL AND METHODIUS UNIVERSITY
FACULTY OF CIVIL ENGINEERING
gf.ukim.edu.mk

RESPONSE SURFACE METHOD ANALYSIS OF ULTIMATE CAPACITY OF INTELLIGENT COMPOSITE ANCHORING ELEMENT

AUTHORS

Štefaňák Jan

Ing. et Ing., Ph.D., researcher / lecturer

Brno University of Technology, Faculty of Civil Engineering, Institute of Geotechnics, Veveri 331/95, 60200, Brno, Czech Republic,

stefanak.j@fce.vutbr.cz

Miča Lumír

Assoc. Prof., Ing., Ph.D., researcher / lecturer/ Head of department

Brno University of Technology, Faculty of Civil Engineering, Institute of Geotechnics,

mica.l@fce.vutbr.cz

The article deals with analysis of transfer mechanism of the force from composite bolt to rock surroundings. The ultimate capacity of anchoring member depends on relatively wide range of input parameters. Moreover, the range of parameters of rock mass changes. The axisymmetric FEM of problem was constructed in Plaxis2D. The Mohr-Coulomb failure criterion, described by equivalent rock strength parameters determined by fitting an average linear relationship to the curve representing Hoek-Brown failure criterion, was used. Later, statistical analysis based on the design of experiment concept and the Response Surface Method (RSM) was carried out. The result of the full-factorial design and RSM analysis provide the regression model. It describes dependence of the bolt ultimate capacity Fy and corresponding deformation uy on the uniaxial compressive strength and Rock Quality Designation RQD. Results show that RQD starts to have significant impact on the Fy from the level of σc above approx. 80 MPa. The deformation uy is affected by the RQD conversely.

Keywords: Fiber Reinforced Polymer, Design of Experiments, Response Surface Method, Pull-out resistance.

1. INTRODUCTION

The amphibolite rock slope of height 10 m was considered in analysis, where the bolt is planned to be used as the anchoring member of passive flexible stabilizing system anchored to the ground, preventing the falling of rock to the railway. Stabilizing systems are formed by membranes, made of cable nets or wire meshes and bolts anchored to the ground (Blanco-Fernandez, 2011). For both types of system, the proper anchoring of their components to the ground is crucial. Different kind of steel rebars is commonly used as tendon of rock bolts. However, steel is susceptible to the corrosion and oxidation and it is not possible to prevent corrosion in long term. Further, steel rebar´s penchant to conduct electrical fields, which makes it

undesirable in application for applications near to the railways with electrically powered vehicles. The reparation or replacement of damaged members is very expensive and problematic. Therefore fiber-reinforced polymer (FRP) rebars can serve as a good alternative to the steel rebars. FRP rebar is the composite material made of the fibers oriented in one direction, which are in thermoset polymer matrices. It won´t rust or corrode, it is also immune to road salt and it is inherently nonconductive, so it won´t interfere with the operation nearby electrical devices. The research aimed on development of the "intelligent" anchoring element (which will be able to monitor changes in its axial strain strain induced e. g. falling stones stopped by wire mesh etc. and immediately inform the responsible office about this change) has been launched in 2016 in Czech Republic. One part of the research is aimed on analysis of the pull-out capacity of those elements. The use concept of Response surface method (RSM) was adopted in this study to illustrate the effect of known factors, that affect the result. The analyzed process of pulling-out the bolt of ground was modelled using the Finite Element Method (FEM). Concept of combination FEM and RSM was used for geotechnical problem previously e. g. by (Wong, 1985) for the slope stability analysis or later by (Lin, 2016) to predict the facing deformations of geosynthetic-reinforced wall.

2. METHODS

2.1 FINITE ELEMENT MODEL OF EXPERIMENT

The Plaxis software 2D has been employed for FEM modelling of the pullout resistance for non-prestressed FRP rock bolt with diameter 20 mm inserted in the gravity grouted borehole of 30 mm diameter. The bond length of bolt was 1.0 m and the whole length is inserted into the cement grout. The bolt has been modelled vertically positioned to achieve the condition of axisymetry. The mesh of 2D 15-noded triangular finite elements with fourth order interpolation of displacement ad twelve Gauss points for the numerical integration has been employed along the embedded length of the bolt. Displacement controlled loading at the anchor head has been adopted. The contact between the anchoring element body and surrounding rock have been modelled by the interface finite elements, which are implemented in Plaxis R_{inter} = 0,9.

2.2 MATERIAL MODELS AND INPUT PARAMETERS OF FRP TENDON AND ROCK MASS

The GFRP tendon of bolt was modelled using linear elastic model with modulus of elasticity of FRP material $E_{f,m}$ = 50 GPa. Poisson´s ratio of FRP tendon was considered 0,2 according to (Mustafa, 2017). Strength and deformation characteristics of the tendon are summarized in the Table 1. The grout body was modelled by the linear elastic model with the value of E_{28} = 15 GPa.

The Mohr-Coulomb (M-C) material model was chosen for simulation of rock behaviour. The M-C strength parameters have been obtained by balanced fitting the Hoek-Brown (H-B) failure criterion by the M-C linear failure line. Material constant m_b of H-B criterion is a reduced value of the intact rock parameter m_i, which also depends on the Geological Strength Index (GSI) (Hoek, 2002) and the Disturbance Factor (D). The value of D was estimated D = 0.7 according (Hoek, 2012). Input parameters are summarized in Table 2. The rock quality, or else core recovery parameter, was evaluated by determination the Rock quality designation (RQD) according (Dere, 1967), which is a rough measure of the degree of jointing or fracture in a rock mass, measured as a percentage of the drill core in lengths of 10 cm or more. The value of Geological strength index (GSI) was then estimated according the correlation presented by (Hoek, 2013):

$$GSI = \frac{52\frac{J_r}{J_a}}{\left(1+\frac{J_r}{J_a}\right)} + \frac{RQD}{2} \quad (1)$$

This relationship is based on the above mentioned RQD and on quotient J_r/J_a included in the Tunnelling Quality Index Q (Barton, 1974). This quotient represents the roughness and frictional characteristics of the joint walls or fillings. The balanced fit was then done by fitting an average linear relationship to the curve representing H-B failure criterion for a range of minor principal stress values defined by $-\sigma_t < \sigma_3 < -\sigma_{3,max}$. This led to the derivation of M-C equivalent effective strength parameters φ´ and c´. The closed form solutions for both the Generalized H-B and the M-C criteria have been used by (Hoek, 2002) to generate hundreds of solutions and to find the value of $\sigma'_{3,max}$, which determination is crucial to conduct above mentioned fitting. For the case of slopes, using Bishop´s circular failure analysis for a wide range of slope

geometries and rock mass properties this analysis gave:

$$\frac{\sigma'_{3max}}{\sigma_{cm}} = 0,72\left(\frac{\sigma'_{cm}}{\gamma H}\right)^{-0,91} \quad (2)$$

where σ_{cm} is the global rock mass strength. The value of Young´s modulus of intact rock E = 107 GPa (Lambe, 1969) was reduced in calculation according to (Hoek, 2006) taking the D and GSI into account, in order obtain a representative stiffness of the in-situ rock mass. Poisson´s ratio of intact rock was estimated by value 0.29. It is in accordance with (Lambe, 1969), where it is reported in range 0.28 – 0.30.

Table 1. Properties of GFRP tendon

Tensile strength (mean value)	$f_{t,m}$	1100	MPa
Tensile strength (characteristic value)	$f_{t,k}$	1050	MPa
Modulus of elasticity	$E_{f,,m}$	50	GPa
Poisson´s ratio	v	0.2	-
Density	ρ	2100	kg/m^3
Nominal diameter	$d_{,nom}$	18	mm
Diameter with adhesion layer	d	20	mm

Table 2. Properties of rock from geological survey

Density of intact rock	γ	2869	kg/m^3
Joint alteration and clay fillings	J_a	0.75	-
Joint roughness factor	J_r	2	-
Uniaxial compressive strength	σ_{ci}	36÷92	MPa
Rock Quality Designation	RQD 0÷1m	57	%
	RQD 1÷2m	36	%
	RQD 2÷3m	24	%

2.3 DESIGN OF EXPERIMENTS AND RESPONSE SURFACE METHODOLOGY

Design of Experiments (DOE) was used to process the results of previously described FEM calculations. This methodology is based on fractional or full factorial experiments, in which the studied design variables are altered at different levels in a systematic way, while the statistical significance of analysis is ensured. It can be seen an alternative way to full-probabilistic design (in the sense of consider randomness of input parameters into design) in the case, where the full information about the probability distribution of input parameters is not available and only few point realizations are known. The term experiment is defined in this concept as the systematic procedure carried out under controlled conditions to illustrate the effect of known factors, that affect the result. In presented study the experiment was conducted numerically. Factors, also called inputs, can be generally classified as either controllable or uncontrollable variables of analysed process. Hence, factors are predictor variables, also called independent variables, which are changed in systematically way during experiment to determine their effect on the response (also called dependent or output, variable) (Box, 2005). The influence of two factors RQD and σ_c on the response has been analysed. The ultimate carrying capacity F_y and corresponding displacement of bolt head u_y were considered as response. Both two factors were referred to as low, intermediate and high level. Three-level full factorial design 3^k was written. It means that *k* factors are considered, each at three levels. The experiment design matrix is written in Table 3.

3. RESULTS

The design pattern of three-level two-factor full factorial design is shown in the Table 3, where the treatment combinations are in the standard order. Randomizing the standard order is not necessary, because the experimental variability does not appear in the numerical experiment. Replication of treatment was also not considered for the same reason. The two last columns of Table 3 are added to the pattern and contain the calculated responses. The linear model with interactions describing the dependence between predictors and response was evaluated. The relationships (3) and (4) represent the resulting regression functions describing analysed dependence.

Table 3. Experiment design matrix with the resulting F_y and u_y

Run Order	Pt Type	Blocks	RQD [%]	σ_c [MPa]	F_y [kN]	u_y [mm]
1	1	1	57	36	29	0,6
2	1	1	57	62	30	0,8
3	1	1	24	36	26	0,9
4	1	1	57	92	44	1,0
5	1	1	36	36	24	0,7
6	1	1	36	62	36	0,9
7	1	1	36	92	43	1,1
8	1	1	24	62	30	0,9
9	1	1	24	92	34	1,0

Diagnostical parameters, that serve for evaluation the efficiency of regression analysis, are summarized in the Table 4 for both models.

Table 4. Estimated regression coefficients for Fy and uy

Term	F_y			u_y		
	SE_coef	T	P	SE_coef	T	P
Constatnt	10,1767	1,963	0,107	0,16678	6,141	0,002
RQD	0,2463	-0,305	0,773	0,00041	-2,979	0,031
σ_c	0,1511	0,883	0,418	0,00025	-0,077	0,941
RQD* σ_c	0,0037	0,821	0,449	0,00006	2,112	0,088

The contour plots and also the 3D surface plots were created to explore the relationship between three variables (two independent factors RQD and σ_c) and the response F_y (Figure 1) and u_y (Figure 2). Contour plots display the 3-dimensional relationship in two dimensions, with x and y factors (predictors) plotted on the x and y scales and response values represented by contours. A contour plot can be seen as a topographical map in which x, y and z values are plotted instead of longitude, latitude and elevation.

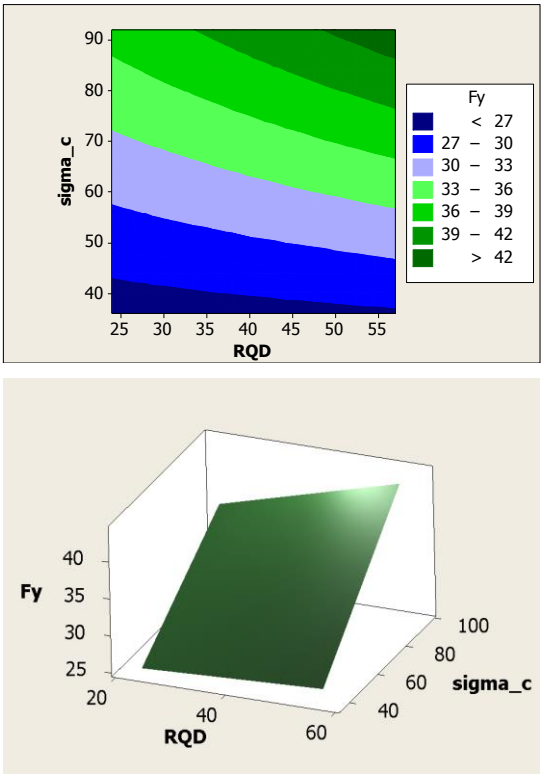

Figure 1. Contour and Surface plot of the ultimate carrying capacity F_y vs σ_c; RQD

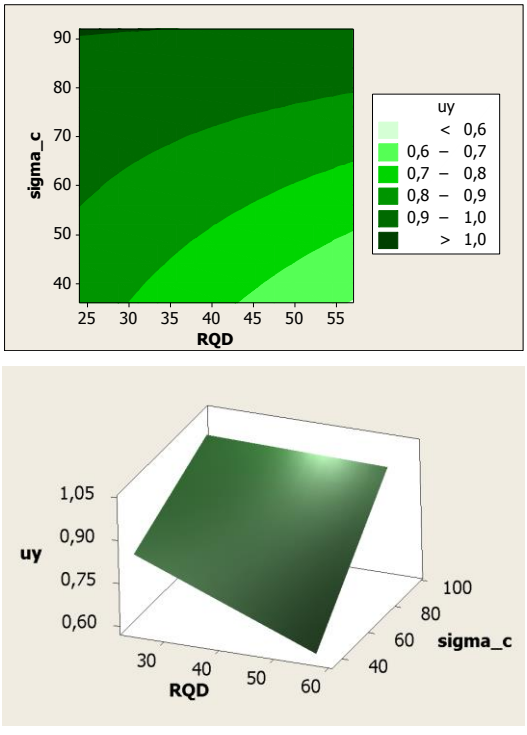

Figure 2. Contour and Surface plot of the deformation measured at the bolt head u_y vs σ_c; RQD

4. DISCUSSION AND CONCLUSIONS

The mathematical-statistical models have been formulated using RSM, in which two factors with three levels were implemented. RQD and σ_c has been chosen as factors, and consequently as the main input parameters of FEM model of rock bolt. The ultimate carrying capacity F_y and corresponding displacement uy of bolt head were followed up output responses. The statistical package MINITAB was used to design and analyze the results of numerically (FEM) calculated experiments. The following conclusions and recommendations can be drawn from the analysis:

• The available geological survey characterizing the rock by determination the RQD values was available. Although there was relatively lack amount of information in the survey applicable directly as input parameters for numerical modelling, there are possibilities how to calculate them cautiously using available correlations. The RQD values was thus transformed to the GSI, which serves as the input for the H-B constitutive model. As the exhausting formulation of the calculation model of bolt was not the task of study, the H-B failure criterion was balanced by the M-C failure line in the range of stresses expected in the analysed slope. The M-C material model with equivalent strength parameters was consequently used for simulation of rock behaviour.

• The linear statistical model with interactions, describing the dependence between predictors and response, was evaluated after finishing all runs of FEM calculation. The statistical significance of the coefficients evaluated on the significance level $\alpha = 0,05$, are summarized in Table 4. The regression was more successful in the case of the model of for uy, where the lower p-values were achieved. It should be noted that in case of F_y the coefficients were statistically insignificant on the chosen level α. The percentage of variation $R\text{-}S_q$ in the response that is explained by the model was $R\text{-}S_q(F_y) = 84,75$ % and $S_q(u_y) = 90,33$ %. The use of higher order models (linear + squares and full quadratic) was analysed also, but it led to the over-fitting the model. It was accompanied by the lower $R\text{-}S_q$, which represents the percentage of variation in the response that was explained by the model. The statistical significance of squared combination of predictors was lower, which was indicating by higher p-values calculated in ANOVA. The full potential of DOE methodology cannot be utilized in experiments based on numerical simulations (e. g. some statistical tests exploring experimental variability) because the experimental variability does not appear in this type of simulations. Although this fact, it still has a significant contribution to effective designing and conducting experiments that leads to a reduction the number of tests needed.

• The results of analysis prove the expected qualitative estimate: the bigger values of RQD and σ_c, the bigger ultimate forces F_y are achieved. The contour and surface plots graphically illustrate those results. Above that, it can be deduced from those plots, that the RQD starts to have higher impact on the ultimate force Fy from the level of σ_c approx. 80 MPa. The deformation uy is affected by the RQD conversely (RQD has bigger impact on results below the level of σc approx. 80 MPa). The numerical results gave deeper insight into the quantitative impact of every considered factor on the monitored response. The ultimate force and corresponding deformation of the bolt is calculated in the form of the range of interval. It is more realistic result, especially in the case of weathered rock massifs, than taking the single deterministically designed value into account.

• Regardless of simple constitutive models, this initial study confirmed the usability of the DOE and RSM concept for the examination and illustration of the effect of factors that affect the response of calculation. Their usefulness will be more obvious, when the more advanced material models and more factors (e. g. different bond lengths or pressure grouting) will be included in the mathematical models. The three-level design was used in case of this study. It is prohibitive in terms of the number of runs, and thus in terms of cost and effort. For example, the two-level central composite design with centre points is much less expensive in case of more considered factors, while it is still a very good way to establish the presence or absence of curvature in case of more factors affecting the response, or in case of more time-consuming calculations. When the proper calibration of the appropriate FEM model will be done, e.g. via the comparison with the results of the full-scale tests that are planned in next phases of the research project, the stronger statistically significant regression relationships can be derived by the RSM concept. Those can then

serve as the kind of design formulas for the design of resistance of analysed bolts.

Acknowledgements

This research was financially supported by the research project No. FV10505 of Ministry of Industry and Trade of the Czech Republic and project LO1408 AdMaS UP of Ministry of Education, Youth and Sport of the Czech republic - Programme of Sustainability I.

REFERENCES

[1] Barton, N., Lien, R. and Lunde, J. (1974). Engineering classification of rock masses for the design of tunnel support. Rock Mech. 6(4), 182-239.

[2] Blanco-Fernandez, E., Castro-Fresno, D., Díaz, J.J. and Lopez-Quijada L. (2011). Flexible systems anchored to the ground for slope stabilisation: Critical review of existing design methods. Engineering Geology [online]. Elsevier B.V, 122(3), 129-145.

[3] Box, G., Hunter, J. and Hunter, W. (2005). Statistics for experimenters: design, innovation, and discovery. 2nd ed. Hoboken, N.J.: Wiley-Interscience.

[4] Dere, D., Hendron, A., Patton, F. and Cording, E. (1967). Design of surface and near surface constructions in rock. Proc. 8th U.S. Symp. Rock Mechanics. NY: AIME American Rock Mechanics Association, s.237-302.

[5] Hoek, E., Carranza-Torres, C. and Corkum, C. (2002). Hoek-Brown failure criterion - 2002 edition. In: Proceedings of NARMS-TAC Conference. Toronto, s. 267-273.

[6] Hoek, E., Carter, T. and Diederichs, M. (2013). Quantification of the Geological Strength Index Chart. In: 47th U.S. Rock Mechanics/Geomechanics Symposium. American Rock Mechanics Association.

[7] Hoek, E. and Diederichs, M.S. (2006). Empirical estimation of rock mass modulus. International Journal of Rock Mechanics and Mining Sciences [online]. 43(2), 203-215.

[8] Hoek, E. (2012). Blast Damage Factor D: Technical note for RocNews - February 2,2012. Winter 2012. https://www.rocscience.com/documents/pdfs/rocnews/winter2012/Blast-Damage-Factor-D-Hoek.pdf.

[9] Kim, M.K. and Lade, P.V. (1984). Modelling rock strength in three dimensions. International Journal of Rock Mechanics and Mining Sciences. 21(1), 21-33. Lambe, T. and Whitman, R. (1969). Soil mechanics. New York: Wiley. ISBN 978-047-1511-922.

[10] Lin, B., Yu Y., Bathurst, R. and Liu, C. (2016). Deterministic and probabilistic prediction of facing deformations of geosynthetic-reinforced MSE walls using a response surface approach. Geotextiles and Geomembranes. 44(6), 813-823.

[11] Mustafa, S. and Hassan, H. (2017). Behavior of concrete beams reinforced with hybrid steel and FRP composites. HBRC Journal [online] DOI: 10.1016/j.hbrcj.2017.01.001.

[12] Wong, F. (1985). Slope Reliability and Response Surface Method. Journal of Geotechnical Engineering. ASCE, 111(1).

EVALUATION OF STRENGTH AND DEFORMATION CHARACTERISTIC PARAMETERS FOR BOULDER CLAY AT SGGW CAMPUS CONSIDERING TEST LOCATION

AUTHORS

Rabarijoely Simon

PhD., Warsaw University of Life Sciences – SGGW, Nowoursynowska 159, 02-776 Warszawa, Poland,

simon_rabarijoely@sggw.pl

Garbulewski Kazimierz

Prof. PhD., Warsaw University of Life Sciences – SGGW

kazimierz_garbulewski@sggw.pl

The selection of soil parameters suitable to the geotechnical design calculations is regarded widely as one of the most important and simultaneously difficult engineering task, which according to the EC 7 should be undertaken into distinct three steps. The second of these steps requires careful and caution estimation with application of the statistical methods even by using a Bayesian approach as shown in this paper. It presents the process of selecting a characteristic strength and deformation parameters from CPT and DMT investigation for boulder clays found in SGGW Campus (Warsaw). This layer was chosen for foundations of design academic buildings. In the selection of the characteristic parameters with application of the numerical program BAYANAL the spatial distribution was taken into account. Particular attention was focused to the affect resulting from in situ test locations at different distances from the design facilities. Finally, the remark conclusions were presented including an approach with weights proposed to determination of the conclusive characteristic values.

Keywords: Characteristic soil parameters, Statistical analysis, Bayesian approach.

1. INTRODUCTION

In geotechnical design with respect to Eurocode 7' rules and principles (EN 1997-1, 2) the step selection of geotechnical actions and resistances (Fig. 1), particularly characteristic material parameters, is considered as a crucial process creating the difficulties for designers. For selecting characteristic values of geotechnical parameters (step 2) the statistical methods are commonly recommended (Frank et al. 2004). The results of this step are affected by many factors, e.g. the uncertainty parameters that

can be derived from natural variability, measurement errors and statistical uncertainty. In the classic statistics, based on a random sample drawn from the population, to determine the average value and standard deviation value with the required confidence level (e.g. 95%) a finite set of values derived from geotechnical parameters population is assumed. In this approach the parameters' values are particular though not known. If we are dealing with a homogeneous medium (ground), to determine the characteristic values of geotechnical parameters ( ) the Student's t-95 percent confidence level can be used according to the formula:

$$X_k = X_m\left[1 - k_n V_x\right] \tag{1}$$

where: X_m - average of soil parameter; k_n - statistical factor; V_x - coefficient of variation. Schneider (1990, 1997, 2010) and Schneider and Fitze (2009) proposed to assume k_n =0,5, it means one half a standard deviation below the mean value. The procedure for determination of characteristic value is presented in Fig. 1, where n is the number of samples, and x_i - parameters in a homogeneous layer.

In an alternative approach, derived from the Bayes' theorem (Alén 1998, Alén and Sällfors 1999, Uzielli 2008), deduction can be based not only on a random sample but also on so-called a priori information. To determine the characteristic values, e.g. strength and deformation of soils, it is proposed to use Bayesian analysis, in which there is possible to continue data collection parameters derived according to the following formula:

$$f(\theta \mid x) = \frac{f(x \mid \theta) \cdot f(\theta)}{\int_{\Omega} f(x \mid \theta) \cdot f(\theta) d\theta} \tag{2}$$

where: f(θ|x) – the posterior density function of q parameter, after the sample's result x has been observed; f(θ) - a priori distribution density function of q parameter; f(x|θ) – credible function i.e. density function of conditional observation's result x with given value of θ; Ω – the set of θ parameter's possible values. The presented Bayes' theorem gives a valuable practical possibility of successive including of new information, coming from consecutively drawn random samples. On a consecutive step, the knowledge about posterior θ parameter's distribution is treated as a priori knowledge of this parameter. An order of including new portions of information does not affect a final result. Bayesian method is preferred when you want to include an objective a priori information about the parameter. You cannot use the classical approach, where only analyzed a random sample taken. it is also preferred the use of Bayesian approach, when we gradually turn to the analysis of a new data set (the idea of observation methods), for example, it can help you in choosing the number of probes required to obtain a satisfactory precision of the data.

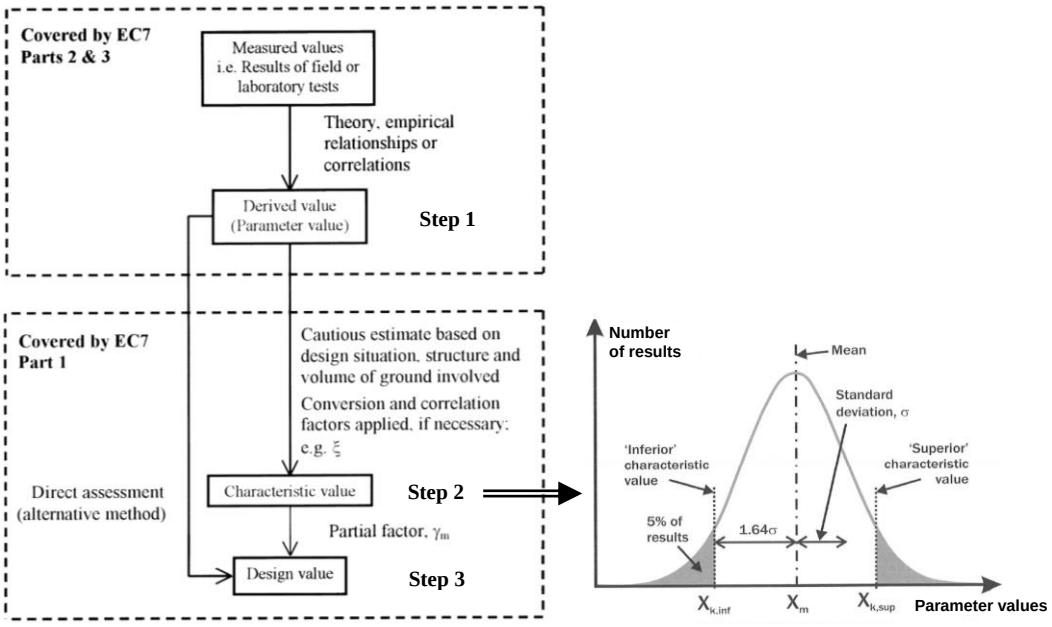

Figure 1. Process for obtaining design parameter values from test results (acc. to Bond and Harris 2008, Orr 2005, Garbulewski et al. 2009).

The paper addresses the applicability of the Bayesian approach to determine a characteristic parameters of boulder clays in geotechnical design of the SGGW Campus in Warsaw. The selection of the geotechnical characteristic parameters was carried out using the new numerical code called BAYANAL. Overview of BAYANAL code, its assumption and requirement and procedure of statistical analysis had been presented. In order to document the impact of in situ test localization the design calculations for selection of characteristic parameters for boulder clay layer in design building on the SGGW Campus were carried out. Finally, the code application in evaluation of characteristic parameters (strength and deformation) for boulder clay was describe.

2. BAYANAL CODE - ASSUMPTIONS AND REQUIREMENT

The basic assumptions and requirements for the BAYANAL code application are as follows: (1) full integration with Excel 2003 (or higher) operating in a Windows environment, (2) intuitive graphical interface, (3) the ability to automatically test of the null hypothesis ("H 0") on the normal random variable on the basis of individual tests samples. Due to the first two requirements it was chosen implementation of applications based on the Excel spreadsheet in 2003 with the support code in Visual Basic for Applications, and a system of MS Office object libraries (libraries Visual Basic for Applications and Microsoft Office Object Library version 11.0). Application forms/dialog boxes with a comprehensive description of the buttons and functions associated with them, depending on the context and the currently executed thread in the application, provided a clear and intuitive graphical interface. All calculations required to perform the analyses are conducted by the formula written on a permanent basis to work spread-sheet (invisible to the user). All input data required for the calculation of the iteration is copied to that worksheet to complete separation of data sources and applications. The procedure in BAYNAL code consists of 3 main steps as follows:

Step 1:

- provide initial data by the user, including the ability to select automatic operation,
- specify the file (s) to the data by the user (standard window opening set),
- open of the first file, activate the first sheet.

Step 2:

- identify (or waiting indication) data to analyze the parameters of initial,
- analyse of the data indicated, any error handling specified data range,
- construct of the Shapiro-Wilk test for a random sample indicated, the term action in the event of non-compliance with the Shapiro-Wilk.

Step 3:

- go to the next test / sheet / file in interactive mode or automatic,
- transit to the report generated by the resignation of the opening of the next set of statistical analysis (“Cancel” button in the dialog box to open files),
- close the source files (with the option: skip shift) and the creation of the report.

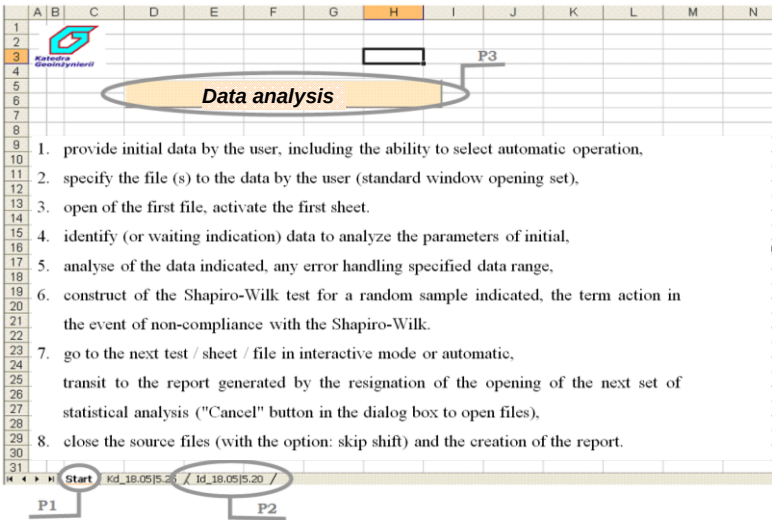

Figure 2. Main sheet of the BAYANAL code

The main sheet of the BAYNAL code is the sheet "Start" (Field 1 - P1) as shown in Fig. 2. The BAYNAL code also includes reports previously performed statistical analyses name" and "date" (no year), and "time" of the analysis and formatted as shown in the P2. Sheets reports of the analyses can move, copy and delete according to standard Excel commands. The work begins with an application of the button P3, constituting of one sheet (P2). The names of these sheets are created automatically according to the scheme: "analysed parameter.

3. SGGW CAMPUS – GEOTECHNICAL CONDITIONS

The geotechnical characteristics of grounds in the buildings designed in the frame of SGGW Campus development were recognized by the interpretation of boring data (102 boreholes), CPT & DMT tests (69 and 41 profiles, respectively) and comprehensive laboratory investigation. Analysing data gathered in the Ground Investigation Report, five geotechnical layers were identified in the campus test site (Fig. 3a), including a layer of brown glacial boulder clay noted in this paper as layer No. III (acc. to geotechnical classification sandy clay - saCL and sasiCL) of the Warta glaciation (gQpW), for which liquidity index values IL = (0.0÷0.11) and a layer of grey glacial boulder clay of the Odra glaciation (gQpO), sandy clay with boulders as layer No. IV, for which IL = (0.0÷0.12). The layer III was pointed out as layer with the most comfortable geotechnical conditions for foundation of the Campus buildings, among them building No 34 analysed in this paper. The distribution of strength and deformation parameters for boulder clay were determined based on CPT and DMT investigation and common used in practice relationships (Fig. 3b).

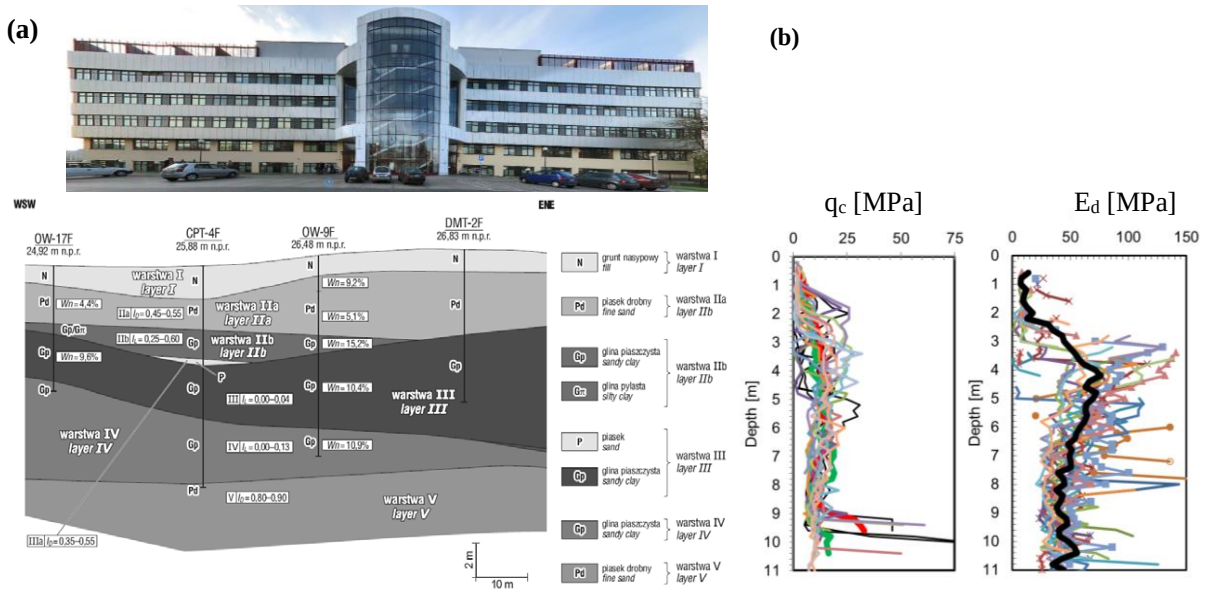

Figure 3. (a) Typical geotechnical cross section for building No 34; wn –moisture, ID – relative density, IL – plasticity index, 23.66 m - meter at Vistula level; (b) Distribution of cone resistance qc of CPT tests and parameter ED based on DMT tests performed on the SGGW Campus

4. SGGW CAMPUS – GEOTECHNICAL CONDITIONS

The BAYANAL code (Garbulewski et al. 2009) was applied to determine the strength and deformation characteristic parameters of boulder clay (layer No III). Because of the availability of all test data both the classical and Bayesian approach could be used. Moreover the characteristic parameters were evaluated according to the Schneider's formula. Taking into account all qc values from CPT tests and Ed from DMT tests (Fig. 3b) for boulder clay in layer No III the characteristic strength (τ_{fu}) and deformation (M – constrained modulus) parameters were calculated as follows:

From classical and Bayes approaches respectively:

τ_{fu} = 0.208 MPa (average value) with standard deviation s_d ± 0.003 MPa;
τ_{fu} = 0.213 MPa (with confidence coefficient = 0,95);
M = 137.4 MPa (average value) with s_d ± 27 MPa;
M = 150.4 MPa (with confidence coefficient = 0,95).

Based on the Schneider formula (2009): τ_{fu} = 0.202 MPa with standard deviation s_d ± 0.012 MPa; M = 124.0 MPa with standard deviation s_d ± 27 MPa.

In order to determine the impact of the test location on the characteristic values of geotechnical parameters (τ_{fu} and M), a statistical analysis was carried out assuming the weight values of the parameters. To determine the weighted values of the parameters the following formula is proposed:

$$\overline{X}_k = \frac{\sum_{1}^{n} x_i \cdot w_i}{\sum_{1}^{n} w_i} \quad (3)$$

where: $\overline{X}_k$ – average weighted geotechnical parameter; x_i - value of the geotechnical parameter; w_i – the weight of the geotechnical parameter as the ratio of the smallest distance from the object and the distance from the remaining tests.

The values of weights for the analysed building No 34 (Fig. 4a) were in the following range: 0,27÷ 1,0 for CPT and 0,43 ÷ 1.0 for DMT. The smallest distance of CPT and DMT location from the design building No 34 were 20.77 m and 31.25 m respectively, however the largest distance were 77.07 m and 73.13 m.

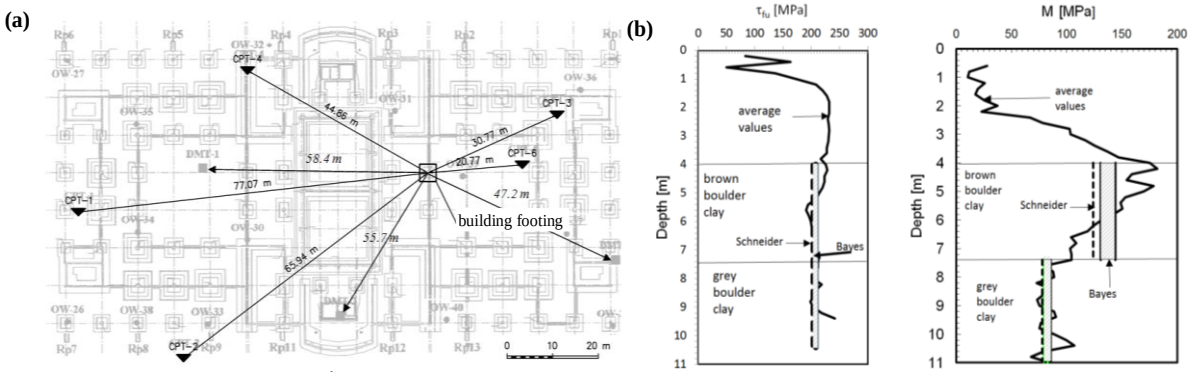

Figure 1. (a) Location of CPT and DMT tests at SGGW Campus (building No 34). (b) Characteristic values of undrained shear strength τ_{fu} and constrained modulus M recommended for geotechnical design

Taking into account q_c values from CPT tests (6 profiles) and E_D from DMT tests (3 profiles) for boulder clay in layer III only for building No 34 the characteristic strength τ_{fu}) and deformation (M) parameters were as follows:

From classical and Bayes approaches: τ_{fu} = 0.210 MPa (average value) with standard deviation s_d ± 0.014 MPa (classical approach) and ± 0.003 MPa (average deviation in Bayes approach at confidence coefficient = 0,95); M = 136.2 MPa (average value) with standard deviation s_d ± 30 MPa (classical approach) and ± 7.5 MPa (average deviation in Bayes approach at confidence coefficient = 0,95). Using the Schneider formula: τ_{fu} = 0.203 MPa with standard deviation sd ± 0.014 MPa; M = 136.0 MPa with standard deviation s_d ± 30.0 MPa.

After introducing weights for parameters from the classical and Bayes approaches the strength and constrained modulus are as follows: τ_{fu} = 0.120 MPa (average value) with standard deviation s_d ± 0.004 MPa (classical approach) and ± 0.001 MPa (average deviation in Bayes approach at confidence coefficient = 0,95); M = 89.0 MPa (average value) with standard deviation s_d ± 19 MPa (classical approach) and ± 4.6 (average deviation in Bayes approach at confidence coefficient = 0,95). Using the Schneider formula: τ_{fu} = 0.118 MPa with standard deviation sd ± 0.004 MPa; M = 79.4 MPa with standard deviation s_d ± 19.1 MPa.

5. CONCLUDING REMARKS

In order to select the deformation and strength parameters for the weakest layer - boulder clay (^{g}QpW), occurring in the ground under the B34 SGGW building statistical analysis of in-situ tests results was carried out. The analysis used indicator parameters (q_c and E_D) from 6 CPT soundings and 3 DMT tests. The mean value, the value with the specified confidence level of 95% and the standard deviation of the indicative parameters were determined using BAYANAL program. In order to take into account the location of in situ tests (test distances from the designed foundation) weights were introduced. The weights were defined as the ratio of the distance close to the

foundation and the distance to the remaining soundings.

The values of the characteristic parameters (τ_{fu}, M) obtained for a single object (B34) are generally comparable with the values of the characteristic parameters obtained for the total area of the SGGW Campus. The strength and constrained modulus parameters of boulder clay recommended for design calculation (lower estimation) obtained using the classic and Bayes approaches and the Schneider formula are as follows respectively: τ_{fuk} 0.206 MPa, 0.207 MPa and 0.203 MPa, M_k 106 MPa, 129 MPa and 121 MPa. The characteristic values of τ_{fuk} and M_k obtained using the weight parameters are distinctly smaller: τ_{fuk} respectively 0.116 MPa, 0.119 MPa and 0.118 MPa, M_k respectively 70.0 MPa, 84.4 MPa and 74.4MPa. These parameter are too conservative taking into account the boulder clay states and preliminary measurements of building settlements.

It is important to underline that to determine the characteristic values of geotechnical parameters statistical methods should be used with caution. The BAYANAL code will be helpful in designing and therefore should be recommended to apply in geotechnical practice.

REFERENCES

[1] Alén C.G. (1998). On probability in geotechnics. Random calculation models exemplified on slope stability analysis and ground-superstructure interaction. Doctoral thesis, Chalmers University of Technology.

[2] Alén C.G., Sällfors G.B. (1999). Uncertainties in modeling of soil properties. Barends et al. (eds), Proc. of the EC SMGE: Geotechnical Engineering for Transportation Infrastructure, Balkema, Rotterdam: 303-308.

[3] Bond A.J., Harris A.J. (2008). Decoding Eurocode 7. Taylor and Francis, London.

[4] EN 1997–1: 2004: Eurocode 7 – Geotechnical design, Part 1: General rules.

[5] Frank R., Bauduin C., Driscoll R., Kavvadas M., Krebs Ovesen N., Orr T.L.L., Schuppener B. (2004). Designers´ Guide to EN1997-1, EC7: Geotechnical design Part 1: General rules. Thomas Telford. London.

[6] Garbulewski K., Jabłonowski S., Rabarijoely S. (2009). Advantage of Bayesian approach to geotechnical designing. Annals of Warsaw University of Life Sciences – SGGW. Ann. Warsaw Univ. of Life Sciences – SGGW, Land Reclam., No 41(2), s. 83 -93.

[7] Orr T.L.L. (2005). Proceedings of International Workshop on Evaluation of Eurocode 7. Department of Civil, Structural and Environmental Engineering, Trinity College, Dublin. 2005.

[8] Schneider H. R. (1990). Die Wahl der Baugrundkennwerte in: Anwendung der neuen Tragwerksnormen des SIA im Grundbau, Mitteilungen der Schweizerischen Gesell-schaft für Boden und Felsmechanik, Zürich.

[9] Schneider H. R. (1997). Definition and determination of characteristic soil properties, XIV ICSMFE, Hamburg, bBalkema, Rotterdam.

[10] Schneider H. R. (2010). Characteristic Soil Properties for EC7: Influence of quality of test results and soil volume involved. Proc. 14th Danube-European Conf. on Geotechnical Eng., 2nd June, 2010, Bratislava.

[11] Schneider H. R. and Fitze P. (2009). Charakteristische Baugrundwerte: Erfahrung, Versuchswerte und Statistik, Herbsttagung SBGF, 6. Nov. 2009, EPFL Lausanne.

[12] Uzielli M. (2008). Statistical analysis of geotechnical data, Geotechnical and Geophysical Site Characterization, Huang & Mayne (eds), Taylor & Francis Group.

PERFORMANCE OF LIQUEFACTION ASSESSMENT METHOD BASED ON COMBINED USE OF CONE PENETRATION TESTING AND SHEAR WAVE VELOCITY MEASUREMENT

AUTHORS

Bán Zoltán

M.Sc., Ph.D. student

Budapest Uni. of Technology, Műegyetem rkp. 3, Budapest, 1111;

ban.zoltan@epito.bme.hu

Mahler András

Ph.D., Assoc. Prof.

Budapest Uni. of Technology,

mahler@mail.bme.hu

Győri Erzsébet

Ph.D., Sr. Res. Fel.; MTA CSFK GGI Kövesligethy Radó Seism. Observatory, Budapest;

gyori@seismology.hu

Empirical liquefaction potential assessment is generally based on the results of CPT, SPT or shear wave velocity (VS) measurement. In more complex or high-risk projects CPT and VS measurement are often performed at the same location commonly in the form of seismic CPT. However, combined use of both in-situ indices in one single empirical method has been limited. After the compilation of a case history database, the authors have developed a combined probabilistic method where the results of CPT and VS measurement can be used in parallel. The goal of this paper was to evaluate the prediction capability of the developed equation on an independent dataset of the 2010-2011 Canterbury Earthquake Sequence and to compare it with commonly used empirical procedures. It was found that the error index defined to quantify the false predictions is the largest for the recommended method but regarding the number of false predictions, it outperforms the other methods used for comparison.

Keywords: Liquefaction, CPT, Shear wave velocity, Prediction

1. INTRODUCTION

Soil liquefaction is one of the most devastating secondary effects of earthquakes and can cause considerable damage in the built infrastructure. Several approaches exist to quantify this hazard. The in-situ test based empirical methods are the most commonly used in practice. Traditional means of these tests are the Standard Penetration Test (SPT), Cone Penetration Test (CPT) and shear wave velocity (VS) measurement. In more complex or high-risk projects, CPT and VS measurement are often performed at the same

location, commonly in the form of Seismic Cone Penetration Test (sCPT). However, even if the results of the two tests are available for the same spot, empirical liquefaction potential evaluation can be performed using either of them, but combined use of the data in one single method has been limited. In order to surmount this issue, an attempt has been made to develop an empirical method, which exploits both the results of CPT and the VS measurement. The effort is based on the assumption that these soil properties complement each other since they characterize the behaviour of granular systems at different levels of strain.

2. LIQUEFACTION POTENTIAL ASSESSMENT BASED ON CONE PENETRATION TESTING AND SHEAR WAVE VELOCITY MEASUREMENT

Since the introduction of cyclic shear stress approach (Seed and Idriss 1971), several empirical methods have been published by different authors that can give a relatively reliable quantification of liquefaction hazard by determining factor of safety or probability of liquefaction occurrence. In current engineering practice, the most commonly used CPT-based methods are the procedures proposed by Robertson and Wride (1998), Moss et al. (2006), Idriss and Boulanger (2008) and Boulanger and Idriss (2014). As the use of CPT for ground profile characterization is very popular, its application for liquefaction potential evaluation is also prevalent.

Since the introduction of cyclic shear stress approach (Seed and Idriss 1971), several empirical methods have been published by different authors that can give a relatively reliable quantification of liquefaction hazard by determining factor of safety or probability of liquefaction occurrence. In current engineering practice, the most commonly used CPT-based methods are the procedures proposed by Robertson and Wride (1998), Moss et al. (2006), Idriss and Boulanger (2008) and Boulanger and Idriss (2014). As the use of CPT for ground profile characterization is very popular, its application for liquefaction potential evaluation is also prevalent.

3. LIQUEFACTION POTENTIAL ASSESSMENT BASED ON CONE PENETRATION TESTING AND SHEAR WAVE VELOCITY MEASUREMENT

3.1 FIELD CASE HISTORY DATASET

The first and most time-consuming step of the development was the collection of a liquefaction/non-liquefaction field case history catalogue. Through careful review of existing CPT and VS databases, 98 cases were found where both measurements are available. As locations where liquefaction occurred are more enticing for post-earthquake field investigators than sites where no apparent liquefaction occurred, the assembled dataset over represents liquefied sites (68 sites), relative to non-liquefied sites (30 sites). The core of the database was assembled from the CPT case history catalogue of Moss et al. (2006) and VS dataset of Kayen et al. (2013), from which 73 and 53 locations could be used, respectively. Additional case histories were gathered from the publications of various authors. For complete list of the used literature, see Bán et al. (2016). The final database consists case histories from 12 earthquakes (1975 Haicheng, 1976 Tangshan, 1979 Imperial Valley, 1981 Westmoreland, 1983 Borah Peak, 1987 Elmore Ranch, 1987 Superstition Hills, 1989 Loma Prieta, 1999 Chi-Chi, 1999 Kocaeli, 2008 Achaia-Elia, 2011 Great Tohoku).

3.2 INPUT PARAMETERS AND THEIR NORMALIZATION

According to the framework of simplified empirical procedures, the seismic demand induced by an earthquake can be represented by the cyclic stress ratio (CSR). This parameter is generally corrected to 7.5 magnitude and 1 a.t.m. effective vertical stress to take into account duration – or number of equivalent cycles – of different earthquakes and the dependency of cyclic liquefaction on effective overburden stress. For these corrections, the method and equations of Idriss and Boulanger (2008) was followed.

Effective overburden stress can also profoundly influence CPT measurements. This effect is typically accounted for by normalizing the tip resistance measured at a given depth to a reference effective stress of 100 kPa. Similarly to CSR, the procedure recommended by Idriss and Boulanger (2008) was followed to take into account this effect. The role of

fines on liquefaction susceptibility is a somewhat contentious topic. Nevertheless, it is agreed that if the fines content (FC) exceeds approximately 35-40% the coarser grains will "float" in the matrix of fine-size particles and the cyclic behaviour of the soil will be governed by the fines. For the development of the equation, equivalent clean sand values of the tip resistance were determined using the updated equation of Boulanger and Idriss (2014). As well as CPT tip resistance, VS is also routinely normalized to an equivalent value measured at 100 kPa effective overburden stress. VS measurement is not capable of detecting small differences in fines content, i.e. VS is relatively insensitive to FC. Compared to uncertainties arising from other parts of the methodology this correction would be fairly negligible; thus, fines content correction of the shear wave velocity was neglected.

After performing all of the above discussed normalization and corrections, three explanatory variables remained to participate in the logistic regression: the equivalent clean sand value of normalized overburden corrected cone tip resistance (q_{c1Ncs}), the overburden corrected shear wave velocity (V_{S1}), and the magnitude and the effective stress corrected cyclic stress ratio ($CSR_{M=7.5,\sigma'v=1atm}$).

3.3 LOGISTIC REGRESSION

Logistic regression is often used to explore the relationship between a binary response and a set of explanatory variables. The occurrence or absence of liquefaction can be considered as binary outcome and the previously summarized three parameters are the explanatory variables. The key components of the regression are the formulation of a limit state model that has a value of zero at the limit state and is negative and positive for liquefaction and non-liquefaction cases, respectively, and a likelihood function that is proportional to the conditional probability of observing a particular event assuming a given a set of parameters. The approach of Cetin et al. (2002) was adopted to form the limit state function.

Assuming the statistical independence of the observations compiled from different sites, the likelihood function can be written as the product of the probabilities of the observations. As it was noted in section 3.1, the dataset contains significantly more liquefaction cases than non-liquefaction cases; this bias is undesirable in logistic regression and can adversely affect the result. A way to address this issue is to weight each class of cases according to the proportion of the other's class population in the total database (Cetin et al. 2002). After taking the natural logarithm of the likelihood function that is more convenient to work with, the unknown parameters were determined using maximum likelihood estimation.

3.4 PROBABILITY OF LIQUEFACTION

The logistic regression using the likelihood function yielded the following result:

$$P_L = \theta\left[\frac{0.080\cdot V_{S1}+0.177\cdot q_{c1Ncs}-8.40\cdot ln\left(CSR_{M=7.5,\sigma'_v=1atm}\right)-46.04}{3.46}\right] \quad (1)$$

where Θ is the standard normal cumulative probability function. The denominator, that is the standard deviation of the error term, is of particular interest since it describes the efficiency of the liquefaction relationship. The regressed value is somewhat higher than that of other commonly used methods, but the method is still promising, since this method has seen little refinement so far. The cyclic resistance ratio for a given probability of liquefaction can be expressed by rearranging Equation 1:

$$CSR_{M=7.5,\sigma'_v=1atm} = exp\left[\frac{0.080\cdot V_{S1}+0.177\cdot q_{c1Ncs}-46.04+3.46\cdot\theta^{-1}(P_L)}{8.40}\right] \quad (2)$$

This can be used in deterministic analysis by selecting a probability contour (typically PL= 15%) to separate liquefaction and non-liquefaction states. Figure 1 shows the probability surface corresponding to PL = 50%.

More detailed description of the complied dataset and the development the above equations can be found in Bán et al. (2016).

4. 2010-2011 CANTERBURY EARTHQUAKE SEQUENCE

The 2010–2011 Canterbury earthquake sequence began with the 4 September 2010 M_w 7.1 Darfield earthquake and included up to ten events that induced liquefaction. However, most notably, widespread liquefaction was induced by the M_w 7.1, 4 September 2010 Darfield and the M_w 6.2, 22 February 2011 Christchurch earthquakes. The ground motions from these events were recorded across Christchurch and its environs by a dense network of strong motion stations. Also, due to the severity and spatial extent of liquefaction resulting from the 2010 Darfield earthquake, an extensive subsurface

characterization program took place with over 10,000 CPT soundings (Green et al. 2014).

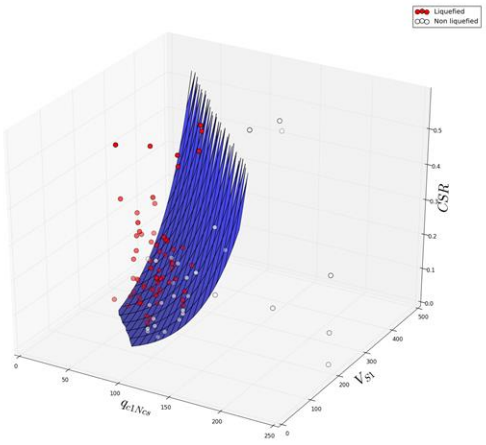

Figure 1. Cyclic resistance ratio surface corresponding to 50% of liquefaction probability (solid squares – liquefaction cases, hollow circles – non-liquefaction cases)

The combination of well-documented liquefaction response during multiple events, densely recorded ground motions for the events, and detailed subsurface characterization provided an unprecedented opportunity to add numerous quality case histories to the liquefaction database. The paper of Green et al. (2014) presented 50 high-quality CPT test liquefaction case histories which consisted of 25 sites analysed for both the Darfield and Christchurch earthquakes. Besides, the compilation of quality liquefaction data, their goal was to compare and evaluate commonly used, deterministic, CPT-based liquefaction evaluation procedures. An error index was used to quantify the overall performance of the procedures in relation to liquefaction observations. It was concluded that among them, the procedure proposed by Idriss and Boulanger (2008) results in the lowest error index for the case histories analysed, thus indicating better predictions of the observed liquefaction response.

In a subsequent research of the same authors (Wood et al. 2017), they examined 46 of the 50 case histories using shear-wave velocity profiles derived from surface wave methods. The VS profiles were used to evaluate the two most commonly used Vs-based simplified liquefaction evaluation procedures (Andrus and Stokoe and Kayen et al.). It was found that the Kayen et al. procedure outperforms the other but has slightly worse performance than that of the CPT-based Idriss and Boulanger method.

The compiled case histories of the Canterbury Earthquake Sequence and the fact that they were explored by both CPT and Vs measurement provide an excellent opportunity for the verification of the developed combined method and comparison with the most commonly used and best performing CPT- and VS-based methods (i.e. with the procedures of Idriss and Boulanger and Kayen et al.).

5. EVALUATION OF PROCEDURES

The papers of Green et al. (2014) and Wood et al. (2017) define an error index to quantitatively assess which liquefaction evaluation procedure yields the "most accurate" prediction for the analysed data. The two error indices used by the two papers are slightly different due to the nature of the CPT- and Vs-based procedures (i.e. the catalogue of the V_S-based method of Kayen et al. didn't have wide enough range to properly account for the K_σ effect). The proposed error indices equal zero if all the predictions correctly match the field observations but increase in value as the number and "magnitude" of the mispredictions increases.

For the present study, a similar concept was adopted to compare the different methods' prediction capability. The aforementioned indices can be illustrated as the vertical distance between the $CRR_{M7.5}$ / $CRR_{M7.5, \sigma'v=1atm}$ curve and the plotted mispredicted point. To allow direct comparison of the methods and to adopt a slightly more straightforward approach, not the vertical distance from the CRR curve were used for quantification, but mispredictions were quantified in terms of factor of safety. On an individual case basis, the error index (EI) equals zero for a correct prediction of a Liquefaction or No Liquefaction case and equals the absolute value of 1 minus FS for mispredicted cases. Similarly to the paper of Wood et al. (2017), to acknowledge the varying significance of the consequences of mispredicting cases, weighting factors are included in the error index: 1.0 for mispredicted liquefaction cases, and 0.5 for mispredicted no Liquefaction cases (Eq. 3).

$EI = 0$ for correct prediction (3)

$EI = FS - 1$ for mispredicted liquefaction case

$EI = 0.5 \cdot (1 - FS)$ for mispredicted no liquefaction case

The computed error index values for the 46 case histories are summarized in Table 1. Please note that the values of error indices are different from those presented in Green et al. (2014) and Wood et al. (2017) due to the different error index definition. Green et al. (2014) and Wood et al. (2017) categorized the cases based on their severity as "no liquefaction", "minor liquefaction", "moderate liquefaction" and "severe liquefaction" cases. For this study, the latter 3 cases were considered as simply liquefaction cases and the first category was obviously the no liquefaction case.

Table 1. Error index and number of mispredicted sites for the three evaluated liquefaction evaluation procedures

Earthquake	Parameter	Idriss and Boulanger (2008)	Kayen et al. (2014)	Bán et al. (2016)
Darfield	Error index	0.731	0.498	1.450
	Number of mispredicted sites	5	3	5
Christchurch	Error index	0.433	0.943	0.711
	Number of mispredicted sites	6	6	2
Total for all sites	Error index	1.164	1.440	2.162
	Number of mispredicted sites	11	9	7

As the table shows the equation of the authors has the highest error index term, so it has the worst prediction capability among the three examined methods. As it is concluded by Wood et al. (2017) and also confirmed by present comparison, the total error values obtained using Kayen et al. (2013) Vs-based procedure is higher than that of the Idriss and Boulanger (2008) CPT-based procedure indicating slightly better performance of the latter method. However, if one considers not the error index but the number of mispredicted sites, in that case the equation recommended by the authors outperforms the other two procedures. The higher error index of the authors' equation is mostly resulted by mispredicted no liquefaction sites for which both the CPT- and V_S-based method predicted liquefaction with factors of safety around 0.6-0.8. As both measurements predicted false response, the recommended formula based on both CPT and V_S also predicted false response but due to the combination of them, its factor of safety is much lower, around 0.3-0.4. On the other hand, during the Christchurch earthquake the CPT- and V_S-based procedures predicted no liquefaction for some liquefied site (FS around 1.0-1.1), for which the recommended combined formula predicted correct response. Due to these factors the recommended combined equation predicted less false responses but where false prediction occurred, the magnitude of error was considerably higher than that of Idriss and Boulanger CPT- or Kayen et al. VS-based method.

6. CONCLUSIONS

More increasingly CPT and VS measurement are often performed on the same location however the possibility to characterize liquefaction potential with both indices in one single empirical method was limited so far. The main goal of the presented research was to develop such a method within the framework of simplified empirical procedures that can reduce uncertainty of empirical methods by combining the two in-situ indices; a small strain property measurement with a large strain measurement. After compiling a case history dataset where both measurements are available and implementing the necessary corrections on the gathered case histories with respect to fines content, overburden pressure and magnitude, a logistic regression was performed to obtain the probability contours of liquefaction occurrence. The proposed formula is an initial attempt to exploit the advantages offered by the measurements of two soil parameters instead of one.

The goal of this paper was to evaluate the prediction capability of the developed equation on an independent dataset of the 2010-2011 Canterbury Earthquake Sequence and to compare it with commonly used empirical procedures. This was performed by means of an error index similar to those defined by Green et al. (2014) and Wood et al. (2017). It was shown that compared to the state-of-

practice CPT-based empirical method of Idriss and Bulanger and VS-based method of Kayen et al., the recommended combined equation of the authors has much higher error index, so it has the worst prediction capability among the three examined methods, but if the number of mispredicted sites is considered, it outperforms the other two procedures. The obtained results are promising, since the author's method has seen very little refinement so far, especially compared to the other two methods.

REFERENCES

[1] Andrus, R.D. and Stokoe, K.H., II. (2000). Liquefaction resistance of soils from shear-wave velocity. Journal of Geotechnical and Geoenvironmental Engineering 126(11): 1015–1025.

[2] Bán Z., Mahler A., Katona T.J. and Győri E. (2016). Liquefaction assessment based on combined use of CPT and shear wave velocity measurement, In: Lehane B.M., Acosta_Martínes A.E. and Kelly. R. (eds), Proceedings of 5th International Conference on Geotechnical and Geophysical Site Characterization, Gold Coast, 5-9 September 2016. pp. 597-602.

[3] Boulanger, R.W. and Idriss, I.M. (2014). CPT and SPT based Liquefaction Triggering Procedures. Report No. UCD/CGM-14/01, University of California, Davis.

[4] Cetin, K.O., Der Kiureghian, A. and Seed, R.B. (2002). Probabilistic models for the initiation of seismic soil liquefaction. Structural Safety 24(1): 67–82.

[5] Green, R. A., et al. (2014). Select liquefaction case histories from the 2010–2011 Canterbury earthquake sequence. Earthquake Spectra, 30(1), 131–153.

[6] Idriss, I.M. and Boulanger, R.W. (2008). Soil Liquefaction during Earthquakes. Monograph MNO-12, Earthquake Engineering Research Institute, Oakland.

[7] Kayen, R., Moss, R.E.S., Thompson, E.M., Seed, R.B., Cetin, K.O., Der Kiureghian, A., Tanaka, Y. and Tokimatsu, K. (2013). Shear-Wave Velocity–Based Probabilistic and Deterministic Assessment of Seismic Soil Liquefaction Potential. Journal of Geotechnical and Geoenvironmental Engineering 139(3): 407-419.

[8] Moss, R.E.S., Seed, R.B., Kayen, R.E., Stewart, J.P., Der Kiureghian A. and Cetin, K.O. (2006). CPT-based probabilistic and deterministic assessment of in situ seismic soil liquefaction potential. Journal of Geotechnical and Geoenvironmental Engineering 132(8): 1032–1051.

[9] Robertson, P.K. and Wride, C.E. (1998). Evaluating cyclic liquefaction potential using the cone penetration test. Canadian Geotechnical Journal 35(3): 442-459.

[10] Seed, H.B. & Idriss, I.M. (1971). Simplified procedure for evaluating soil liquefaction potential. Journal of the Soil Mechanics and Foundations Division 97(SM9): 1249-1273.

[11] Wood, C.M., Brady, R.C., Green, R.A, Wotherspoon R.M., Bradley, B.A and Cubrinovski, M. (2017). Vs-Based Evaluation of Select Liquefaction Case Histories from the 2010-2011 Canterbury Earthquake Sequence. Journal of Geotechnical and Geoenvironmental Engineering 143(9): 04017066.

CRITICAL STATE CONSTITUTIVE MODEL FOR OVERCONSOLIDATED CLAYS – HASP MODEL

AUTHORS

Jocković Sanja

Ph.D., Civ.Eng.

Faculty of Civil Engineering, University of Belgrade, Blvd. Kralja Aleksandra 73, Belgrade, Serbia; borovina@grf.bg.ac.rs

Vukićević Mirjana

Ph.D., Civ.Eng.

Faculty of Civil Engineering, University of Belgrade, mirav@grf.bg.ac.rs

The paper presents a simple critical state bounding surface constitutive model for describing the mechanical behaviour of over consolidated clays. Keeping the simplicity and the same set of the parameters as Modified Cam Clay model, new model provides a more realistic description of numerous elements of clay behaviour. The novel form of the hardening rule was proposed with the state parameter and the degree of overconsolidation as the state variables. Expressing the hardening parameter through the state parameter of the stress point on a loading surface and the state parameter of a conjugate stress point on the bounding surface, strain hardening and strain softening in drained conditions, as well as negative pore pressure in undrained conditions are well described. Inner loading surface always passes through the current stress point, thus enabling elasto-plastic soil behaviour even in early stages of loading. The model overcomes many deficiencies of the Modified Cam Clay model as demonstrated on a broad experimental evidence.

Keywords: Constitutive model, over consolidated clays, state parameter.

1. INTRODUCTION

The development of advanced, but at the same time simple for the use in engineering practise constitutive model for soil, is essential for the rational design of the geotechnical structures. Bearing in mind that simple expressions and clear physical meaning of the model parameters are an imperative for practical application of constitutive models, the Hardening State Parameter model (HASP) for describing mechanical behaviour of over consolidated clays is developed on the basis of the critical state theory and within the concept of bounding surface plasticity (Dafalias and Herrmann 1980). The HASP model overcomes many deficiencies of the Modified Cam Clay model (MCC) (Roscoe and Burland 1968): inadequate predictions of the behaviour on dry side, large elastic region, as

well as sudden transition from elastic region into plastic region. At the same time, HASP model retains the same simplicity and the same set of parameters as MCC model.

2. HASP MODEL

Relations of the HASP model are based on the following principles: soil is isotropic, plastic strains develop from the very beginning of loading, hardening parameter depends on the increments of plastic volumetric and shear strains. Bounding surface is the MCC surface. Point A (p',q) representing the current stress state is always on the inner yield surface, Figure 1a:

$$\frac{p'}{p_0'} = \frac{M^2}{M^2 + \eta^2} \tag{1}$$

Associated flow rule applies, i.e. plastic strain increment vector is always normal to the yield surface.

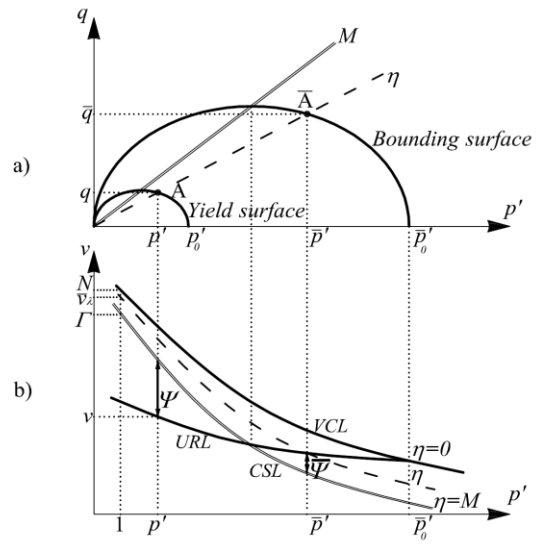

Figure 1. a) Bounding surface concept b) State parameters

Bounding surface possesses all the characteristics of the MCC surface. For stress ratio below the critical state line (CSL), the volume decreases and the surface expands, while for stress ratio above the critical state line, the volume increases and the surface shrinks. Yield surface expands until peak strength is reached at stress ratio η=Mf, after which it shrinks (softening) until critical state is reached.

2.1 HARDENING RULE FOR THE HASP MODEL

Volumetric hardening rule does not allow negative dilatancy to develop for overconsolidated soils before the peak strength is reached. In order for the yield surface to continue expanding also for stress ratio values M<η<Mf, it is necessary to use combined hardening and express the hardening rule as a function of plastic shear strain also (Nova and Wood 1979, Yao et al. 2009) as follows:

$$dp_0' = \frac{v}{\lambda - \kappa} p_0' \left(d\varepsilon_v^p + \xi d\varepsilon_q^p \right) \tag{2}$$

where ξ is a parameter discussed later in the paper, v is specific volume, λ is a slope of the virgin compression line (VCL), κ is a slope of an swelling line (URL) in v-lnp' plane, Figure 1b. The combined hardening significantly affects the stress path. This formulation allows the effective stress path to cross the CSL and reach the peak in drained conditions. In an undrained test, the combined hardening is key to achieve “S” shaped effective stress path. If the plastic shear strain increment is expressed through the dilatancy and if current overconsolidation ratio is defined as:

$$R = \frac{\bar{p}'}{p'} = \frac{\bar{q}}{q} = \frac{\bar{p}_0'}{p_0'} \tag{3}$$

the hardening rule for the yield surface can be written as:

$$dp_0' = \frac{v}{\lambda - \kappa} p_0' d\varepsilon_v^p \left(1 + \frac{\xi}{d} \right) R = \frac{v}{\lambda - \kappa} p_0' d\varepsilon_v^p \omega \tag{4}$$

where ω is the hardening coefficient:

$$\omega = \left(1 + \frac{\xi}{d} \right) R \tag{5}$$

Expressions for plastic strains thus becomes:

$$d\varepsilon_v^p = \frac{\lambda - \kappa}{v} \frac{1}{p'} \frac{1}{\omega} \left(\frac{M^2 - \eta^2}{M^2 + \eta^2} dp' + \frac{2\eta}{M^2 + \eta^2} dq \right) \tag{6}$$

$$d\varepsilon_q^p = \frac{\lambda - \kappa}{v} \frac{1}{p'} \frac{1}{\omega} \left(\frac{2\eta}{M^2 + \eta^2} dp' + \frac{4\eta^2}{\left(M^2 + \eta^2 \right)\left(M^2 - \eta^2 \right)} dq \right) \tag{7}$$

The hardening coefficient is at the same time the reduction coefficient for plastic strains. It is then possible to assume that soil deforms plastically from the very beginning of loading. When peak strength is reached (transition from hardening to softening), applies and maximum gradient of volume change

(negative dilatancy) is noticeable, marked as dmin by the compression-positive convention. Based on Eq. (4) it can be concluded that if ω=0 then i.e. parameter □ is the absolute value of dilatancy at peak strength in drained conditions, which is in line with the considerations stated in Nova (2006).

2.2 STATE PARAMETER

According to works of Parry (1958), Li and Dafalias (2000), Jefferies and Been (2006), dilatancy is not a function of the stress ratio η only, it also depends on the state parameter Ψ. State parameter represents the difference between the current specific volume and the specific volume on the reference state line (CSL) at the same mean effective stress, Figure 1b, (Been and Jefferies 2006). State parameter for the current stress state, i.e. point on the yield surface, can be expressed as:

$$\Psi = v + \lambda \ln p' - \Gamma \tag{8}$$

where Γ is specific volume on the CSL for reference pressure (p'=1kPa). State parameter is negative for highly overconsolidated clays $\Psi < 0$, while for lightly overconsolidated and normally consolidated clays state parameter is positive $\Psi > 0$. When stress point reaches the CSL then $\Psi = 0$. State parameter for conjugate point on the bounding surface can be expressed as:

$$\bar{\Psi} = (\lambda - \kappa) \ln \left(\frac{2M^2}{M^2 + \eta^2} \right) \tag{9}$$

Also, the current overconsolidation ratio via state parameters can be expressed as:

$$R = \frac{\bar{p}'}{p'} = \frac{\bar{q}}{q} = exp\left(\frac{\bar{\Psi} - \Psi}{\lambda - \kappa} \right) \tag{10}$$

In the expression for the hardening coefficient (5) it is necessary to define the ratio □/d. Detailed explanation is given in Jocković and Vukićević (2017) and the following expression for the hardening coefficient is proposed:

$$\omega = \left(1 + \frac{\bar{\Psi} - \Psi}{\bar{\Psi}} \right) R \tag{11}$$

For normally consolidated clays, the HASP model automatically transforms into the MCC model since $\Psi = \bar{\Psi}$ and hardening coefficient is then ω=1.

3. VALIDATION OF THE HASP MODEL

Validation was done against published results of drained and undrained tests in triaxial compression and extension, on the samples with various overconsolidation ratios. The HASP model requires five material parameters for describing stress – strain relations. All the parameters can be easily determined by the conventional laboratory tests and they are summarized in Table 1. Considering that the HASP model is formulated to overcome the basic drawbacks of the MCC model, comparison has been made between experimental results, HASP model and MCC model.

Table 1. Parameters of the HASP model

	λ	κ	M_c	M_e	Γ	μ
Kaolin clay (Biarez & Hicher 1994), CD tests	0.23	0.03	0.81	/	3.44	0.2
Cardiff clay (Banerjee & Stipho 1979), CU tests	0.14	0.05	1.05	0.85	2.63	0.2

The hardening behaviour of Kaolin clay in drained conditions is well predicted by the HASP model for all overconsolidation ratios (OCR=8, 4, 2). For heavily overconsolidated tests, the HASP model predicts a drop in strength – softening, Figure 2a. The dilatant behaviour has been observed and excellent prediction of the change of volumetric strains is achieved, Figure 2b.

Large deviations from experimental results were recorded for the MCC model, especially for high overconsolidation ratio. Peak strength is overestimated up to two times.

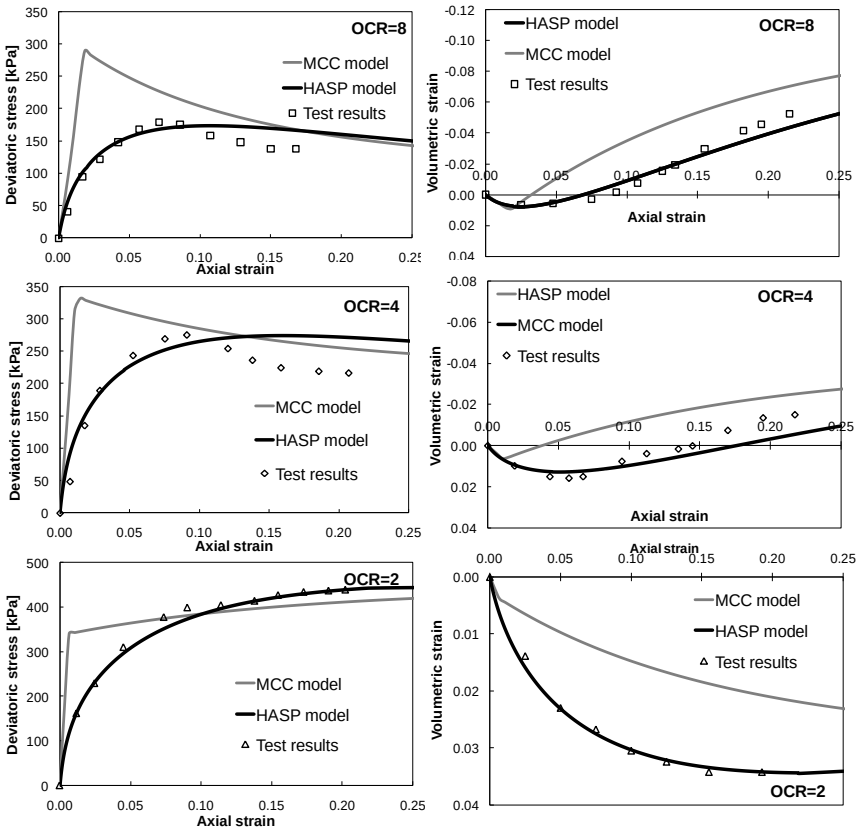

Figure 2. CD tests, Kaolin clay a) Stress-strain relations b) Volumetric strains

Results of two undrained triaxial compression tests for remoulded samples of Cardiff Kaolin clay with overconsolidation ratios 5 and 12 are presented, as well as results of two undrained triaxial extension tests for remoulded samples with overconsolidation ratios 6 and 10. Very good agreement with experimental results is noticeable for HASP model (stress-strain relations – Figure 3 and pore water pressure changes – Figure 4), for all overconsolidation ratios in triaxial compression and extension tests. General form of the effective stress paths (normalized with the equivalent mean effective stress on the VCL) depending on the overconsolidation ratios is well predicted, Figure 5. Disadvantages of the MCC model can be seen in undrained conditions, also.

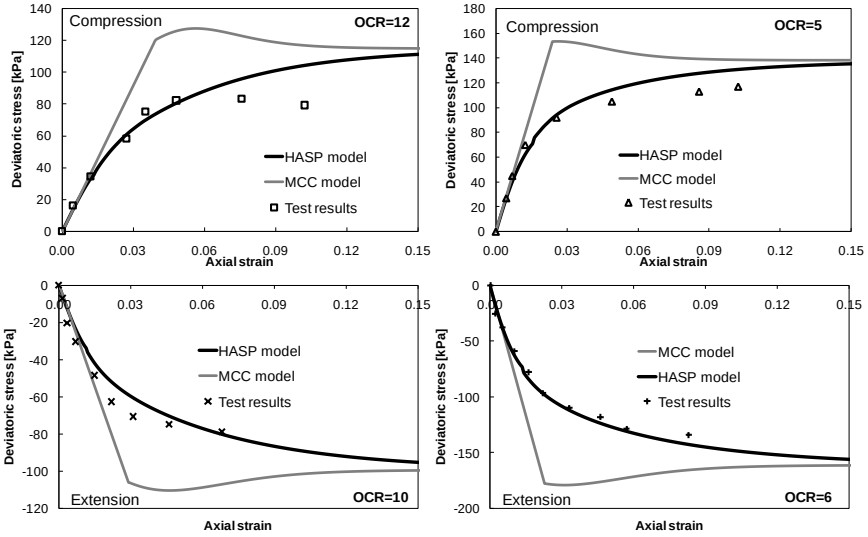

Figure 3. CU tests, Cardiff clay – stress-strain relations

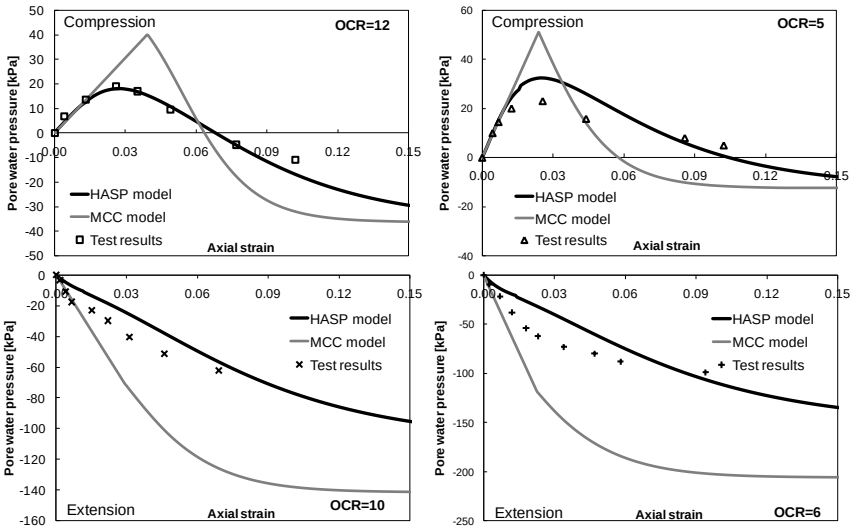

Figure 4. CU tests, Cardiff clay – pore water pressure

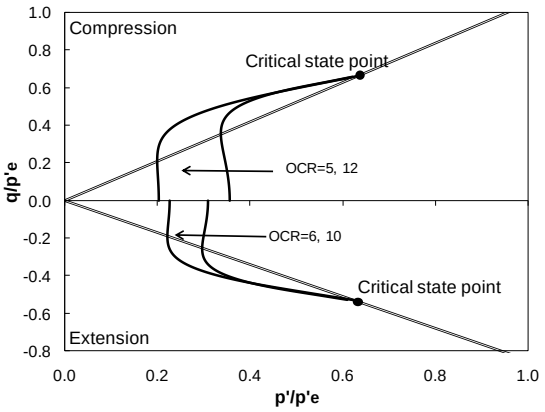

Figure 5. CU tests, Cardiff clay – normalized effective stress paths

4. CONCLUSIONS

With novel form of the hardening rule it is possible to describe a number of elements of the mechanical behaviour of overconsolidated clays. In drained conditions, unlike the MCC model, HASP model predicts the smooth transition from contractive to dilatant behaviour before the peak strength is reached and a smooth transition from hardening to softening, without mathematical description. In undrained conditions, the general form of the effective stress paths depending on the overconsolidation ratio is well predicted, as well as pore water pressure. There is no pure elastic domain, but the hardening coefficient reduces plastic strains depending on the current degree of overconsolidation. For normally consolidated clays the HASP model transforms into the Modified Cam Clay model.

REFERENCES

[1] Banerjee, P.K. and Stipho, A.S. (1979). Elastoplastic model for undrained behavior of heavily overconsolidated clays. Int J Numer Anal Mech Geomech; 3(1): 97-103.

[2] Been, K. and Jefferies, M.G. (1985). A state parameter for sands. Géotechnique, 35(2): 99-112.

[3] Biarez, J. and Hicher, P.Y. (1994). Elementary Mechanics of Soil Behaviour. Saturated Remoulded Soils. A. A. Balkema, Rotterdam.

[4] Dafalias, Y.F. and Herrmann, L.R. (1980). A bounding surface soil plasticity model. Proc. Int. Symp. on Soils under Cyclic and Transient Loading, Vol. 1, Swansea, U.K., 335–345.

[5] Jefferies, M.G. and Been, K. (2006). Soil Liquefaction: A critical state approach. Taylor and Francis, Abingdon.

[6] Jocković, S. and Vukićević, M. (2017). Bounding surface model for overconsolidated clays with new state parameter formulation of hardening rule. Comput Geotech, 83:16–29.

[7] Li, X.S. and Dafalias, Y.F. (2000). Dilatancy for cohesionless soils. Géotechnique, 50:449–60.

[8] Nova, R. and Wood, D.M. (1979). A constitutive model for sand in triaxial compression, Int J Numer Anal Methods Geomech, 3: 255–78.

[9] Nova, R. (2006). Modelling of bonded soils with unstable structure. International Workshop on Modern Trends in Geomechanics – Vienna, Springer.

[10] Roscoe, K.H. and Burland, J.B. (1968). On the generalized stress-strain behaviour of wet clay. Engineering Plasticity, Cambridge University Press, 535 – 609.

[11] Yao, Y.P., Hou, W., Zhou, A.N. (2009). UH model: three-dimensional unified hardening model for overconsolidated clays, Géotechnique, 59:451–69.

MODELS AND CALCULATION METHODS OF THE PILE FOUNDATION IN SCAD OFFICE

AUTHORS

Nuzhdin Leonid

Ph. D., Professor

Novosibirsk State University of Architecture and Civil Engineering, Perm National Research Polytechnic University
Leningradskaya st. No.113 Novosibirsk
Russia
nuzhdin_ml@mail.ru

Mikhaylov Victor

Ph.D. student, Civ.Eng.;

Novosibirsk State University of Architecture and Civil Engineering, Perm National Research Polytechnic University
Leningradskaya st. No.113 Novosibirsk
Russia
vsmikhailov@mail.ru

The authors in this article review different approaches to the simulation of pile foundations using finite element methods and analytical methods, developed in SCAD Office and GeoSoft Software. Problems of ensuring the accuracy of calculations with different detailed elaboration of models of pile foundations are discussed. Special attention is paid to the features for implementing described methods of pile foundation modelling under seismic impacts.

Keywords: Pile foundations, Ground base models, Finite element method, Platform models of pile foundations.

1. INTRODUCTION

In the modern engineering there is a huge experience in calculation of file foundations accumulated on the base of finite elements method. Application of one or another engineering method depends on the construction particularities of a foundation including the degree of the detalization of the calculation in relation to forces in the zone under consideration. Methodologies, contained herein, consider soil structure interaction analysis. They are taken from common practice by the companies, which use the SCAD Office and GeoSoft software for computing foundations of civil objects, as well as specialized programs for the nuclear industry.

We can select three groups of calculation methods for file foundations shown in Table 1. The main group include the analytical methods, which are realized in technical standards of Russian Federation Numerical calculations of file foundations with the use of software, which founded on the method of finite elements, could be divided in two independent groups: bearing static loads and bearing dynamic loads (Table 1). Such division is essential due to foundations the rigidities of which can be changed by the short time dynamic actions. It is also useful to study the singular stress-deformed state of a multi-

storey building in operation stage with account of the genetically nonlinear history of its construction work.

The analytic methods used in the SCAD Office are founded on the results of scientific experiments and theoretic substantiating states. The probable calculation inaccuracies of such methods are connected with admissions in fundamental research and imprecisions of site investigation. If using numerical finite element methods, the maximum possible errors in the form of the absolute extreme deviation from analytic theoretic solutions can be estimated in correspondence with the results of the Table 2. These data were provided during recent certification for solving problems of designing objects of nuclear industry. Examination of the software complex was carried out by A. M. Belostotskii, V.I. Golyakov, A.G. Tyapin, S.A. Toporkov, S.S. Nefedov, S.V. Prokopovich, A.V. Esenov.

There are extreme deviations set out in Table 2, which can be seen in various tests of different types. The given values of the enveloping deviations give an estimate picture, which confirms that the use of direct physical models with solid finite elements for modelling of a soil foundation has the maximal risk of errors accumulation. Due to dynamic calculation the error level of numerical solutions can either increase or decrease depending on the number of minus-plus signs. The compensation of the accumulating error in the direct static and dynamic models of beds in the form of solid finite elements should be carried out with the use of more accurate multi-node finite elements. It is also can be done by doubling the spectrum method with more detailed dynamic calculations in the mode of the direct integration of motion equations with the use of seismograms.

Table 1. Approaches to classification of methods for calculation of pile foundations

Classification of calculation methods	Method for calculation of pile foundations
1. On detalization degree of analytic models	1.1. The discrete model of a pile group.
	1.2. The discrete model of a pile field on the base of the cell method.
	1.3. The conditional foundation on the natural bed in the form of an support plate on the elastic half-space.
	1.4. The pile reinforced ground base with reduced characteristics.
2. On numerical FEM-models in static conditions	2.1. The Winkler foundation with constant contraction coefficient of the bed C_1.
	2.2. The two parameter Pasternak model with the constant coefficients of the bed for contraction C_1 and for displacement C_2.
	2.3. The bilinear Fedorovskey model with variable coefficients of the bed C_1.
	2.4. The direct physical linearly elastic model of the half-space with solid elements.
3. On numerical FEM-models in dynamic conditions	3.1. The dynamic model with constant coefficient C_1 or with variable coefficient C_1 and single-node dampers in the both types.
	3.2. The direct dynamic model in the form of solid finite elements with nonuniform damping and with reflectionless or remote horizontal boundaries.
	3.3. Numerical-analytical platform models.

Table 2. Calculation deviation ratios in using various types of the SCAD finite elements

Types of engineering calculations	Maximum deviations of calculation results in SCAD in verification tests of analytic solutions	
Static calculation of the parameters of the stress-deformed state in the linear option	7%	for rod elements
	10%	for plate elements
	21%	for solid elements
Dynamic calculation of the stress-deformed state	8%	calculation of natural frequencies
	14%	calculation of forces and stresses from dynamic loads

2. 2 ANALYTIC MODELS OF PILE FOUNDATIONS

The discrete model of a pile group, regulated by paras 7.4.4-7.4.5 of the SP 24.13330.2011, based on the research papers of V.G. Fedorovskey, S.N. Levachyova, S.V. Kurillo, Y.M. Kolesnikova. There is a constraint in the SP 24.13330.2011, which said that we should not use more than 25 piles in one group. Nevertheless, in the originating works that methodology was intended to be for the foundations of hydro engineering structures, in which, as distinct from regularly loaded pile fields, unbalanced loading can be seen without constraints of the number of the piles in a group.

In the present methodology a group foundation is regarded as a discrete set of separate piles with unique rigidity characteristics of the bed accounting the horizontal and vertical influences on neighboring piles (Fig. 1). The advantage of this approach is the maximal detailed calculation of forces in each point along the length of any pile and also the clear manifestation of the marginal pile effect on the boundary pile rows and on the corner piles of the group (Fig. 2, a).

As a peculiarity of the pile group method is the necessity to carry out a nonlinear iterative calculation with the account of the vertical mutual influence of the piles in the group and the rigidity of the pile raft. This peculiarity also includes the necessity of carrying out a nonlinear calculation to provide the allowable horizontal normal stresses of soil in the zone of side surfaces contact. Another matter in dispute of the calculation method for the pile foundation as for a pile group is the convention of the linear increasing of the horizontal reduction of a pile shaft by soil. In calculations with long piles it leads to over-estimation of the reactive forces with the increasing reduction of the pile shaft. In addition to that, the horizontal influence of the piles in a group, which decreases the side soil pressure, is verified by the scientific experiment only for cases of the orthogonal mutual alignment of piles and only for sandy soil.

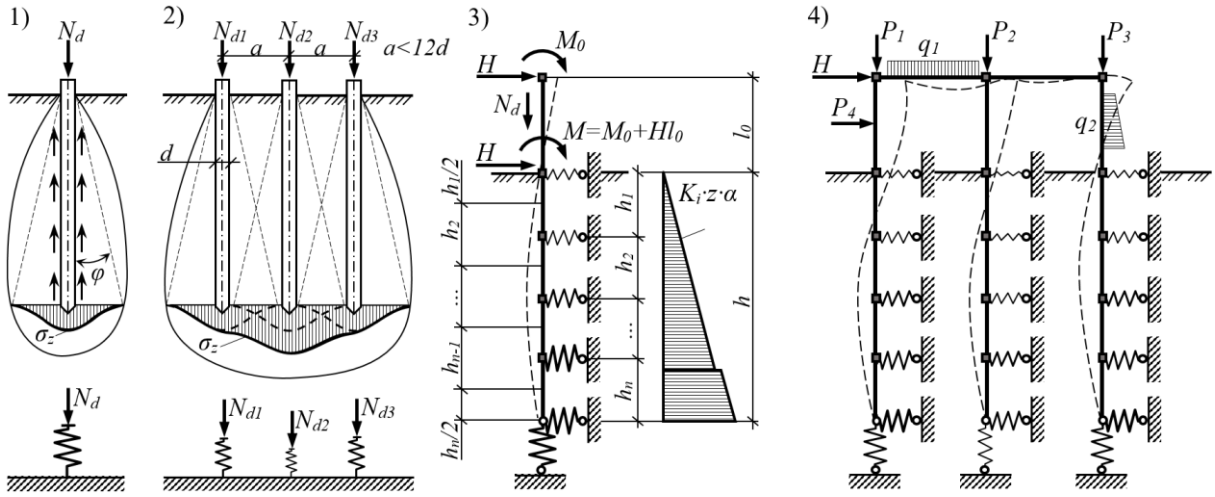

Figure 1. Vertical and horizontal stiffness properties of neighbouring piles

The discrete model of the pile group is more investigated and widely represented in normative documents for dynamic calculations. The account of the decreasing pile capacity on vertical loads is carrying out by introduction of decreasing coefficients in accordance with the SP 24.13330.2011. The partial contact loss of the side surface of a pile with soil in horizontal direction is accounting in accordance with the SP 14.13330.2014. The account of the dynamic properties of soils for pipe foundations in such a quasi-static state is very easy to check by simple equations. The abovementioned decreasing coefficients have been reduced significantly in the research made by V.A. Ilichejv, Y.V. Mongolov, V.M. Shayevich. However, their extended fundamental methodology is more interesting in terms of the maximal detailed computerized calculation and removal of the existing constraints for dynamic calculations. In these calculations the difference of the pile loading level is not accounted in various points of the foundation with the use of uniform coefficients. In addition to that, there is no possibility to use nonlinear calculations with the redistribution of the supporting loads between the field piles or group piles. In this case we take in the account the pile raft flexibility due to inapplicability of

the superposition principle for dynamic calculations.

The discrete model of a pile field on the cell method is described in paras 7.4.6-7.4.9 of the SP 24.13330.2011. The authors of that methodology are the staff under the charge of V.G. Fedorovskii. The advantage of the methodology is the easy for programming with regular disposition of piles and in the account of axial actions in the discrete model of the pile field. Nevertheless, that methodology does not allow to check the strength of the boundary piles, when bending moments arise in them. It should also be taken into account, that the layer summation method does not account the rigidity of the foundation plate in calculation of the mean settlement of the conditional foundation on the central and corner points. As a result, the account of the pile raft rigidity in the model of elastic half-space shall reduce the average settlement, and that can be seen in the methodology. This problem can be solved in the software Geo-Set in shared use with SCAD. In Geo-Set the method of elastic half-space is not solved in a table style but in an explicit form by the spacial integrating of the Boussinesq task (Fig. 3).

The conditional foundation method for a pile field on natural bed (Fig. 2, b) is recommended in para 6.1. of the SNiP 2.02.03-85. In the modern technical standard SP 24.13330.2011 the model of conditional foundation was integrated in the cell method. However, in the engineering practice the modeling method of conditional foundation in the form of a support plate with soft rigidity on an elastic half-space is still popular. This numerical approach is not in conflict with the cell method and it uses the elastic half-space on the border of the contact of the support plate with application of the Pasternak model with two proportionality coefficients. For such a pile foundation model on a support plate at the level of the bottom of the piles at first glance may seem a simple task, the dynamic properties of the base due to making the static stiffness of the Foundation soil to the dynamic stiffness by multiplying by a common factor, regulated in SP 22.13330.2014 in the absence of other data. However, this approach dramatically overestimates the bearing capacity of the piles is observed in experiments decrease, which limits the applicability of the model.

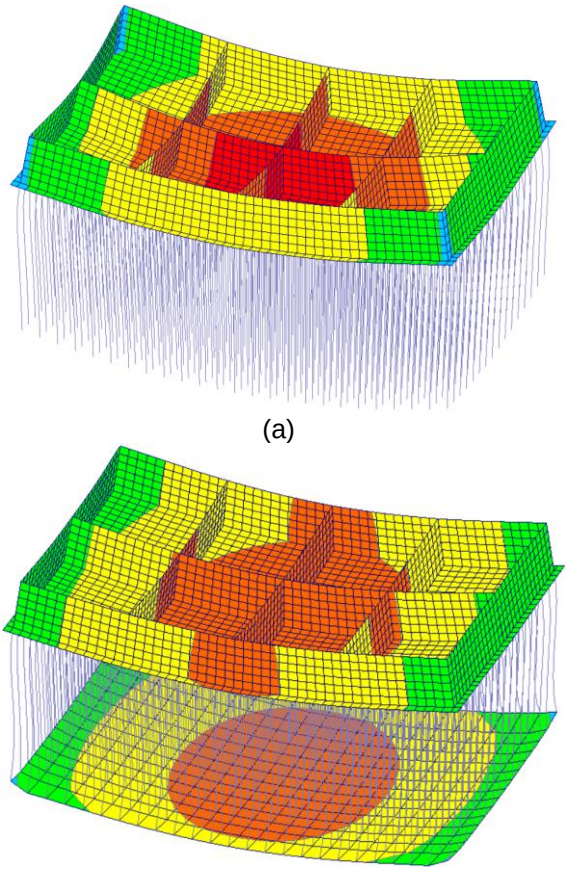

(a)

(b)

Figure 2. The settlement analysis of a pile foundation with the use of the discrete model described in paras 7.4.6-.9 of the SP 24.13330.2011 (a) and conditional foundation model by para 6.1. of the SNiP 2.02.03-85 (b)

A less accurate calculation method is the pile reinforced bed with reduced characteristics. According to the recommendations of the instruction paper “Designing and calculation plate foundation beds with soil-cement columns”, published by the Moscow State Building Construction University, the reduced deformation module of the reinforced bed should be calculated in the form of the direct mean value on the specific area of the soil piles and soil bed in relation to the plate area on the reinforced bed. The model in such a simple form of a pile bed does not allow to receive information about forces in a single pile. Nevertheless, this approach allows to avoid error accumulations in calculation models due to the stress concentrators which take place under the lower pile ends and on the side surface of physic models with solid finite elements. JSC Atomenergoproekt has similar views in designing atomic reactors with pile foundations on weak sub-bases.

According to the soil mechanics the reduced characteristics method can be applied to both pile foundations and combined pile-plate foundations, when it is necessary to prove the state by the result comparison of other prescribed and approved methods. The advantage of the bed model with reduced characteristics is the possibility of stress control in any point of the elastic half-space by the way of special integrating of the Boussinesq task. This method also allows to model beds with heterogeneous soil layers by the way of accounting the corresponding deformation module. An example of calculation of the plate foundation on a pile bed in the Geo-Set Pro software is shown at Figure 3.

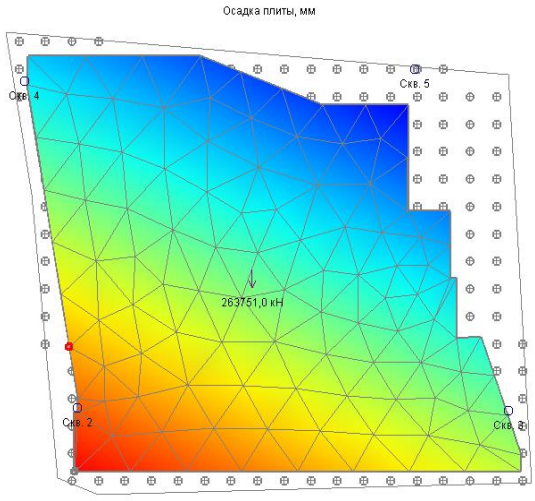

(a)

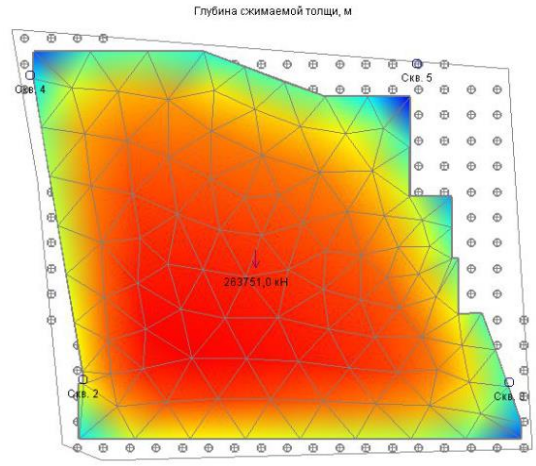

(b)

Figure 3. The settlement analysis of a pile foundation with the use of the discrete model described in paras 7.4.6-.9 of the SP 24.13330.2011 (a) and conditional foundation model by para 6.1. of the SNiP 2.02.03-85 (b)

3. DIRECT PHYSICAL MODELS

It should be mentioned, that physical models are numerical models of the finite element method, in which piles together with soil bed layers are modelled by solid finite elements. Such models have the abovementioned risk of error accumulations on the one hand, but on the other hand they have the pictorial presentation of calculation results and can be used as an auxiliary analytical model for the detailed analysis of a stress-deformed soil state. The auxiliary type of this model is explained by the necessity in calibrations of such models with reduction of settlements and stresses in accordance with expected results provided by proved analytic methods in technical standards. In addition, in the process of performing numerical studies of direct physical models of pile Foundation, it was revealed that they lead to incorrect results, without increasing the horizontal stiffness of the soil in connection with the increase in compression of the body of the pile in the lateral surface of the piles with increasing depth.

If the direct physical model of the pile foundation should experience dynamic impacts, it is necessary to adhere to a number of technological requirements. First, the oscillation damping in soils is much higher than in the concrete. Therefore, in the current version of SCAD functions to account for the inhomogeneous damping of different materials were implemented. Solving such dynamic problems is possible using the module «Direct integration of motion equations». Secondly, during the analysis of vibrations of the base the effect of the reflected waves should eliminated. It could be done by increasing the dimension of the model to the extent when the distance to the boundary edges will be sufficient to fade the reflected waves. Alternatively, it could be done by introducing non-reflecting boundary edges with one-node dampers, implemented in the latest version of SCAD. In terms of dynamic effects direct physical models can have high inaccuracy, as it was previously mentioned in the first paragraph of the article.

4. NONPHYSICAL PLATFORM MODELS

Platform models have now become the international standard for calculations of foundations for the most important facilities of nuclear industry, operating in conditions of

seismic effects. This was preceded by numerous experiments, showing high precision of the platform models in the process of predicting the behavior of real objects in comparison with previous approaches on the use of direct physical models, wave models and the contact dynamic models. Technology create platform models based on the modified asymptotic method combined with the use of four software systems are described in detail in the monographs of A. G. Taypin, chief specialist of JSC "Atomenergoproekt". Integrated translational and rotational springs at the nodes of the foundation base are calculated as the result. These elements of finite stiffness do not have any physical interpretation, but accurately describes the interaction of Foundation and structure.

The combined asymptotic method can be divided into five main stages. In the first stage using the program SHAKE, you move from the original base exposure on the earth's surface with the available accelerograms by deconvolution to the underlying basalt basement of the tectonic plate. Then the engineer executes the reverse convolution to a new designed level of the ground contact with the deepened foundation. In the second stage FEM-calculation of superstructures on a rigid ground base is performed with the definition of the dynamic matrix of inertia in the frequency range. The dynamic matrix of inertia in a single node located at the center of gravity under the sole of foundation slab. In the third step, you should calculate the impedances and transfer functions to seismic loads impacting the foundation on a uniform layered basis, held motionless. The third stage is carried out using software CLASSI for surface foundations or SASSI for deepened foundations. In the fourth stage, using the software AGA new accelerograms are synthesized for the modified and reinforced ground base, allowing to calculate the response of a rigid foundation under a structure with modified properties of soils. In the final step in a finite element analysis program the engineer generates a platform model with transfer functions from foundation vibrations to the impact on the non-physical platform.

5. CONCLUSIONS

In this paper, the authors reviewed five methods of pile foundation modelling in terms of static loads. In the presence of significant seismic effects on structure it is recommended to use the following methods: the discrete model of a pile group or the model of a pile field; the simplified model of the pile reinforced ground base with reduced characteristics; the direct physical model using solid FEM elements, the inhomogeneous damping of different materials and non-reflecting boundary edges; the nonphysical platform model.

On authors` opinion, the combined asymptotic method, based on platform models, deserves the most attention as it was approved for designing foundations under seismic effects for the structures of nuclear industry, attracting the best scientific and engineering technologies. This method should be adapted for mass use in engineering calculations for civil and industrial purposes. In this case the software has to be facilitated to one complex program on the one hand, and the theory as well should be simplified on the other hand.

REFERENCES

[1] Edigarov, G. (2015). Experience in application of SCAD OFFICE in analysis of intermediate double-row pile pier with account of mutual interference of piles. CADMASTER, 3: 88-97.

[2] Evtushenko. S., Krakhmalnyi T. (2017). Investigation of the behavior of strip foundations with complex configuration of the base. Soil Mechanics and Foundation Engineering, 54-3: 169-172.

[3] Fedorovskii. V., Levachev. S., Kurillo. S., Kolesnikov. I. (2003). Piling in hydraulic structures. Izdatel'stvo ASV.

[4] Il'ichev. V., Mongolov. YU., SHaevich. V. (1983). Pile foundations in seismic regions. Strojizdat.

[5] Nuzhdin. L, Mikhaylov. V. (2018). Modeling methods of the system pile foundation–earth foundation in SCAD Office with allowance for mutual influence of the piles. PNIPU Bulletin. Constr. and architecture, 9-1: 113-130.

[6] Petruhin. V., Bezvolev. S., Shuljat'ev. O., Harichkin. A. (2007). Pile-raft foundation analysis with consideration of perimeter pile effect. Urban development and geotechnical construction, 11: 90-97.

[7] Stavnicer, L. (2010). Seismic stability of the ground bases and foundations. Izdatel'stvo ASV.

[8] Tyapin A. (2016). Analysis of structures with regard for subgrade interaction. Izdatel'stvo ASV.

STEREOGRAPHIC PROJECTION FOR TERRITORY OF THE REPUBLIC OF MACEDONIA

AUTHORS

Zlatko Srbinoski
Phd, Full Professor
Ss. Cyril and Methodius University
Faculty of Civil Engineering – Skopje
email: srbinoski@gf.ukim.edu.mk

Zlatko Bogdanovski
Phd, Assistant Professor
Ss. Cyril and Methodius University
Faculty of Civil Engineering – Skopje
email: bogdanovski@gf.ukim.edu.mk

Filip Kasapovski
MSc, Assistant
Ss. Cyril and Methodius University
Faculty of Civil Engineering – Skopje
email: kasapovski@gf.ukim.edu.mk

Tome Gegovski
MSc,
Ss. Cyril and Methodius University
Faculty of Civil Engineering – Skopje
email: gegovski@gf.ukim.edu.mk

In stereographic projection, as one of the oldest cartographic projections, Earth is approximate with sphere in the first step and then it is projected on the tangent or cutting plane. The famous Bulgarian geodetic scientist Prof. Vladimir Hristov Ph.D. made stereographic projection with direct projecting of ellipsoid on plane. In this work, basically postulate for composing of stereographic projection for territory of R. of Macedonia are defined.

Keywords: stereographic projection, linear deformations

1. INTRODUCTION

The stereographic projection is one of the oldest known cartographic projections. This projection for the first time was examined by the Greek astronomer Hiparh (180-125 BC), and Ptolemy (87-125 year), who expounded its main features.

The first application of the stereographic projection for the needs of the state survey on the territory of the Balkans dates back to 1863 when it was first used in the regions that belonged to Austria-Hungary. In the aforementioned projection, first, the Earth's ellipsoid was projected onto a sphere, and then a conformal mapping was made of the sphere onto a plane. In addition, a tangent projection plane is applied to the Earth's sphere at one point - approximately in the middle of the mapped territory. As the point of tangency is the trigonometric point of the Gelerthe Hill, near Budapest, which is at the same time a coordinate beginning of the system, named the Budapest coordinate system.

Due to its good character, the stereographic projection falls within the scope of "geodetic" projections, which are often used as national cartographic projections. This is particularly true for countries that have a territory in a circular shape, for which the stereographic projection gives maximum good results.

Due to these characteristics, the stereographic projection is also part of the world projection system where it is used to display the polar regions and is known as the *UPS projection* – (Universal Polar Stereographic Projection).

2. BASIC CHARACTERISTICS OF THE STEREOGRAPHIC PROJECTION

Stereographic perspective azimuthal projections are projections where the mapping is done on a plane that touches or cuts the Earth's sphere (Figure 1). While mapping, the laws of the linear perspective are used, and the observation point V is located on the terrestrial sphere with radius R. The projection's plane, regardless of whether it is tangent or secant, is always normal to the main diameter Qo V.

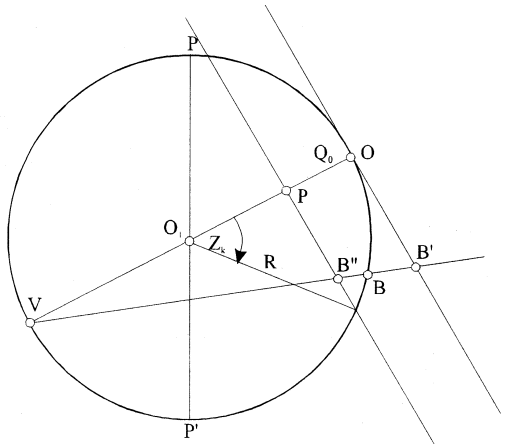

Figure 1. Stereographic projection on tangent, or secant plane

The main diameter in the stereographic projections of the tangent plane is defined by the distance:

$$\overline{VO} = 2R \qquad (1)$$

When a secant plane is applied, corresponding to the main diameter, the distance K is defined, which, according to Figure 1, is:

$$\overline{VP} = K = R(1+\cos z_K) \qquad (2)$$

Slant stereographic projections on the tangent plane represent the general kind of these projections.

The points on the terrestrial sphere are defined by their sphere-polar coordinates: azimuth (A) and zenith distance (z), relative to the pole of the projection Qo (Figure 2).

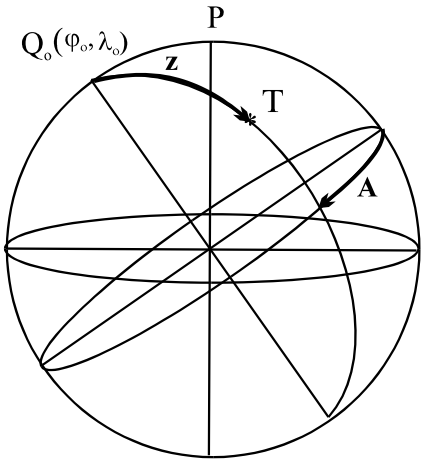

Figure 2. Sphero-polar coordinate system

For the same points in the projection, the polar and the Cartesian coordinates are defined (Figure 3).

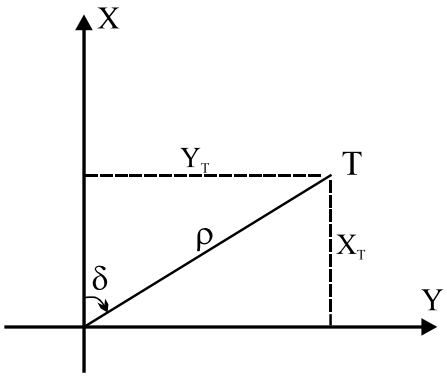

Figure 3. Polar and Cartesian coordinates in the projection plane for point T of the terrestrial sphere

The polar coordinates in the plane (ρ, δ) are defined with the following formulas:

$$\begin{aligned} \delta &= A \\ \rho &= 2R \cdot tg\frac{z}{2} \end{aligned} \qquad (3)$$

The Cartesian coordinates according to (Figure 3) are defined with the following formulas:

$$\begin{aligned} X &= \rho\cos\delta = 2R \cdot tg\frac{z}{2} \cdot \cos A \\ Y &= \rho\sin\delta = 2R \cdot tg\frac{z}{2} \cdot \sin A \end{aligned} \qquad (4)$$

These coordinates can also be expressed in function of the geographical coordinates of point T and the pole Qo:

$$X = \frac{2R\ (\sin\varphi\cos\varphi_0 - \cos\varphi\sin\varphi_0\cos l)}{1+(\sin\varphi\sin\varphi_0+\cos\varphi\cos\varphi_0\cos l)} \quad (5)$$

$$Y = \frac{2R\cos\varphi\sin l}{1+(\sin\varphi\sin\varphi_0+\cos\varphi\cos\varphi_0\cos l)}$$

Where φ_o is the latitude of the pole Qo, φ is the latitude of the point T, and l is the difference between the longitude λ at point T and the longitude λ_o of the coordinate beginning Qo, i.e. : $l = \lambda - \lambda_o$.

The linear deformation module in the direction of the vertical (μ_1) and the almucantar (μ_2) is defined by the formula:

$$\mu_1 = \mu_2 = \frac{1}{\cos^2\frac{z}{2}} > 0 \quad (6)$$

For stereographic projections on secant plane, the linear deformations for points above the secant plane are negative, while for points below the projection plane they are positive. In both cases, the absolute values of the linear deformations grow with distancing from the intersecting circle, called the "zero deformation circuit" (Fig. 4)

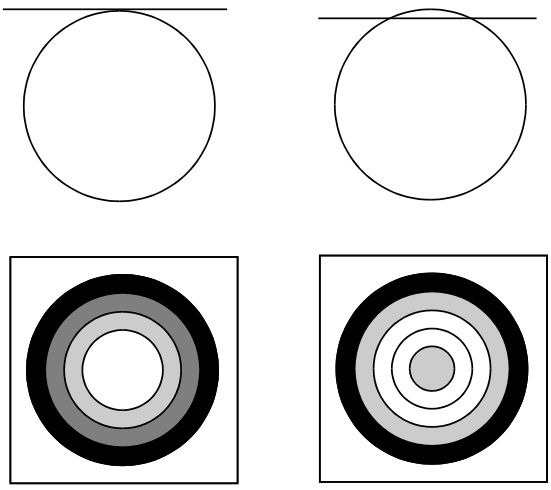

Figure 4. Schematic representation of deformations in the stereographic projection on the tangent and on the secant plane

3. STEREOGRAPHIC PROJECTION ACCORDING TO THE METHOD OF PROF. VLADIMIR HRISTOV

The stereographic perspective azimuthal projection, developed according to the method with constant coefficients (from Prof. Dr. Vladimir Hristov), defines the following geometric characteristics:

- The Earth's ellipsoid is approximated with a sphere.
- The point Qo is the center of the mapped territory, and at the same time it is the point where the projection plane touches the Earth's sphere (Figure 5):

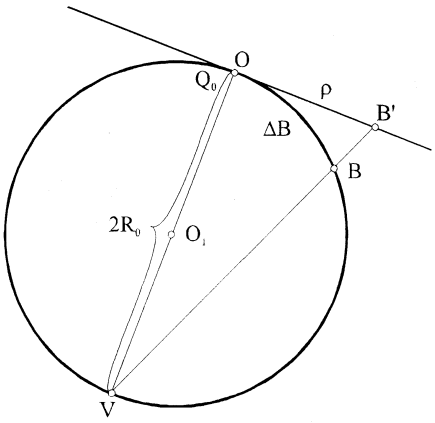

Figure 5. Basic geometric characteristics on the stereographic projection of prof. V. Hristov

- The perspective projection of all points of the Earth's sphere is performed from point V which is found on the opposite side of the Earth's surface.
- The projection is defined as conformal, which means that there are linear and surface deformations, while there are no angular deformations.
- For a coordinate beginning in the projection plane, the point O is adopted, which is the image of the center of the projection Qo. Point O is a coordinate beginning in the system of cartesian stereographic coordinates.
- A meridian with geographical longitude λ_o, which passes down the center of the projection Qo, is mapped as a straight line that is adopted for the X-axis, with a positive direction north. The normal direction to X-axis at Point O is defined as Y-axis in the projection plane.

Having in mind the aforementioned conditions, the expressions for the basic calculations in the stereographic projection can be made.

3.1 DIRECT TASK

The transformation of the geographical coordinates (φ, λ) into Cartesian stereographic coordinates (Y, X) is done by means of expressions with constant coefficients, which depend on the difference in geographical latitudes (Δφ) and the difference on the geographical longitudes (*l*) between the individual projected points and the center of the projection Qo (φ_o, λ_o).

Expressions for calculation are obtained by the method of prof. V. Hristov, according to which all the elements dependent on the geographical latitude φ (such as: the isometric latitude q, the radius of curvature of the parallels r, etc.) are developed in the Taylor series near the center of the projection Qo. The resulting differentials, calculated around the central point, represent constants that are grouped together to give constant coefficients.

In relation of the fact that the stereographic projection is defined as conformal, for this projection are valid Cauchy–Riemann's differential equations that say:

$$x + iy = f(q + il) \tag{7}$$

After the necessary development and differentiation, as well as the separation of the real from the imaginary part, the final expressions for calculating the cartesian coordinates X and Y are obtained:

$$\begin{aligned} X = {} & a_{10}\,\Delta\varphi + a_{20}\,\Delta\varphi^{2} + \ldots + a_{70}\,\Delta\varphi^{7} + \\ & + a_{02}\,l^{2} + a_{12}\,\Delta\varphi\,l^{2} + \ldots + a_{52}\,\Delta\varphi^{5}\,l^{2} + \\ & + a_{04}\,l^{4} + a_{14}\,\Delta\varphi\,l^{4} + \ldots + a_{34}\,\Delta\varphi^{3}\,l^{4} + \\ & + a_{06}\,l^{6} + a_{16}\,\Delta\varphi\,l^{6} + \ldots \end{aligned} \tag{8}$$

$$\begin{aligned} Y = {} & b_{01}\,l + b_{11}\,\Delta\varphi\,l + \ldots + b_{61}\,\Delta\varphi^{6}\,l + \\ & + b_{03}\,l^{3} + b_{13}\,\Delta\varphi\,l^{3} + \ldots + b_{43}\,\Delta\varphi^{4}\,l^{3} + \\ & + b_{05}\,l^{5} + b_{15}\,\Delta\varphi\,l^{5} + \ldots \end{aligned} \tag{9}$$

In the expressions (8) and (9) the coefficients a_{ij} and b_{ij} represent the sum of products of the coefficients a_n and c_n, defined by the expressions:

$$a_n = \frac{1}{n!}\left(\frac{d^n x}{dq^n}\right)_0 = \frac{1}{n!}\,f^n(q)_0 \tag{10}$$

$$c_n = \frac{1}{n!}\left(\frac{d^n q}{d\varphi^n}\right)_0 = \frac{1}{n!}\,f^n(\varphi)_0 \tag{11}$$

The calculation of the coordinates X and Y is most easily performed in a matrix form.

3.2 INDIRECT TASK

The calculation of the second geodetic task, i.e. the calculation of the geographical coordinates (φ, λ) on the rotational ellipsoid, from the given Cartesian stereographic coordinates (Y, X), are also expressed in terms of special constant coefficients. In this case, the coordinate differences Δφ and Δλ are calculated, in relation to the geographical coordinates φ_o, λ_o) and *l*, for the center of the projection Qo. The geographical coordinates φ and λ are determined according to the following formulas:

$$\varphi = \varphi_0 + \Delta\varphi \qquad \lambda = \lambda_0 + l \tag{12}$$

In view of the fact that the conditions for conformal mapping apply, the Cauchy-Riemann differential equation for this transformation is:

$$\Delta q + il = F(x + iy) \tag{13}$$

After the development of the equation in Taylor series, as well as the separation of the real of the imaginary part, the finite expressions are obtained for Δφ and *l*, which have the form:

$$\begin{aligned} \Delta\varphi = {} & A_{10}\,x + A_{20}\,x^{2} + \ldots + A_{50}\,x^{5} + \\ & + A_{02}\,y^{2} + A_{12}\,x\,y^{2} + \ldots + A_{42}\,x^{4}\,y^{2} + \\ & + A_{04}\,y^{4} + A_{14}\,x\,y^{4} + \ldots + A_{06}\,y^{6} + \ldots \end{aligned} \tag{14}$$

$$\begin{aligned} l = {} & B_{01}\,y + B_{11}\,x\,y + \ldots + B_{51}\,x^{5}\,y + \\ & + B_{03}\,y^{3} + B_{13}\,x\,y^{3} + \ldots + B_{33}\,x^{3}\,y^{3} + \\ & + B_{05}\,y^{5} + B_{15}\,x\,y^{5} + \ldots \end{aligned} \tag{15}$$

The coefficients A_{ij} and B_{ij} in the expressions (14) and (15) represent the sum of products with different degrees of coefficients A_n and C_n, defined by the formulas:

$$A_n = \frac{1}{n!}\left(\frac{d^n q}{dx^n}\right)_0 \tag{16}$$

$$C_n = \frac{1}{n!}\left(\frac{d^n \varphi}{dq^n}\right)_0 \tag{17}$$

3.3 LINEAR DEFORMATIONS AND DEFORMATIONS OF LENGHT

The stereographic projection, defined as a conformal projection, possesses the properties that the angles of the terrestrial sphere don't deform in the projections, while the lengths and the surfaces of the mapping are deformed. The linear deformation modulus (μ) in stereographic projections is defined with the formula:

$$\mu = \frac{1}{\cos^2 \frac{z}{2}} \qquad (18)$$

Figure 6 shows the dependence of the deformation modulus μ from the zenith distance z, the arc L, and the radius Ro to the terrestrial sphere.

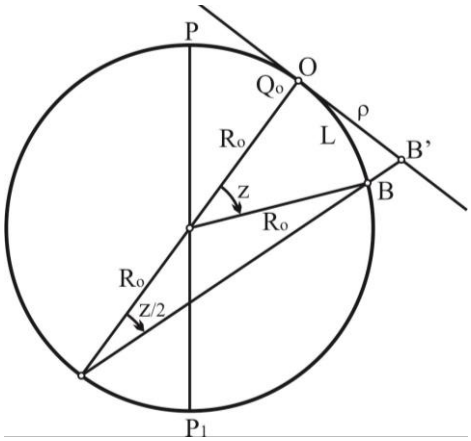

Figure 6. Dependence of the deformation modulus μ from the zenith distance, arc L and the radius R_o on the terrestrial sphere

From the picture is obtained:

$$\frac{z}{2} = \frac{L}{2R_0} \qquad (19)$$

Having this in mind, according to a series of mathematical operations, the linear module of deformations in a finite form reads as follows:

$$\mu = 1 + \frac{L^2}{4R_0^2} \qquad (20)$$

The definitive expression for the calculation of the relative linear deformations (D_t), according to the expression (20), takes the form:

$$D_T = \mu - 1 = \frac{L^2}{4R_0^2} \qquad (21)$$

$$D_T = \mu - 1 = \frac{\rho^2}{4R_0^2} = \frac{X^2 + Y^2}{4R_0^2} \qquad (22)$$

In the expression (22) X and Y are the Cartesian stereographic coordinates of point B (Figure 6), for which the linear deformations are calculated.

4. ELEMENTS FOR DEFINING THE STEREOGRAPHIC PROJECTION FOR THE TERRITORY OF THE REPUBLIC OF MACEDONIA

4.1 DEFINING THE CENTER OF THE PROJECTION Q_O

For the definition of the center of the projection (Qo) it is necessary to construct a circle with a minimum radius that will tangent the territory of the Republic of Macedonia in a few extreme points. This is for locating the center of the projection in the middle of the territory that is being mapped, in order to obtain minimal deformation of the lengths in the projection. For this purpose, the auxiliary map in the scale of 1: 1000000 was used and the extreme points defined during the reconstruction of the Tissot's projection in the Republic of Macedonia.

From such a defined basis, the construction of circles, which with the help of translation shifting, is brought in a position to tangent the border line from the territory of the Republic of Macedonia. The circle with a minimal radius touches the boundary line in points 8, 14 and 17 and runs close to points 1, 6, 7, 15 and 16 (Figure 7). The radius of the circle is read from the screen:

ρ_{min} = 108.0 mm (km)

After the establishment of the border circle on the digital basis, the location of the center of circle was determined, which is a coordinate beginning for the stereographic projection of the Republic of Macedonia.

The geographical coordinates of the center of the projection have the following values:

$\varphi_o = 41^o\ 30'\ 30''$ $\lambda_o = 21^o\ 45'\ 50''$

Figure 7 shows the position of the boundary circle and the center of the stereographic projection in relation to the border line from the territory of R. Macedonia.

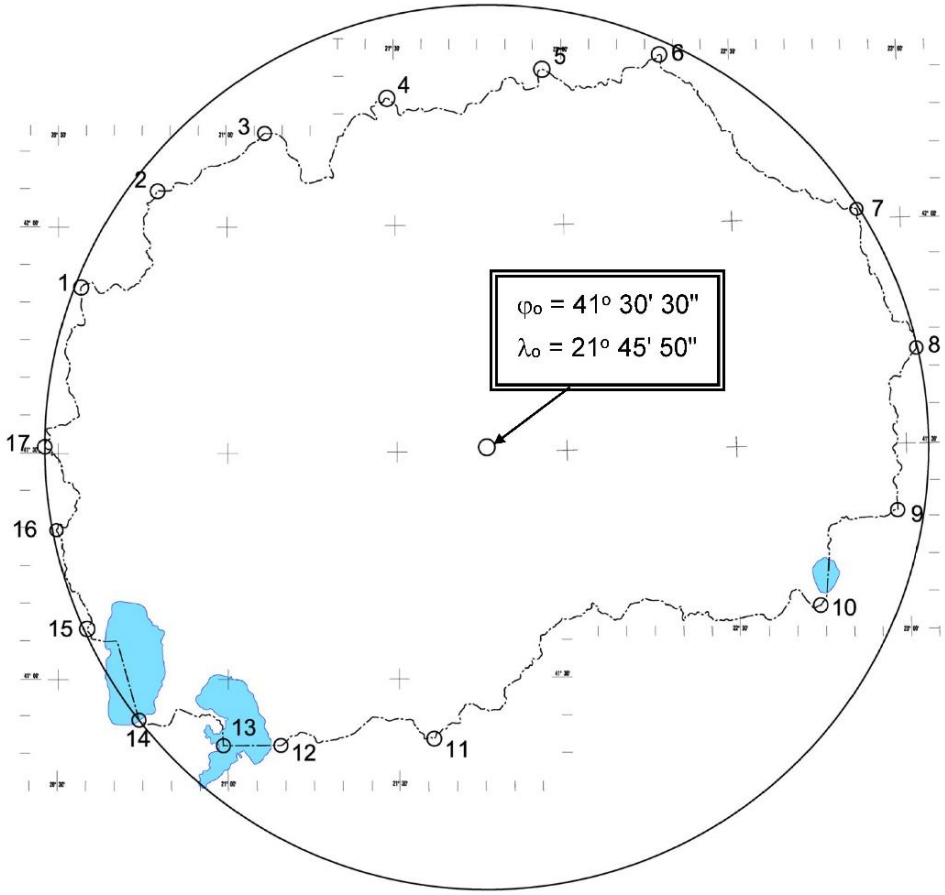

Figure 7. The boundary circle and the coordinate beginning of the stereographic projection of the Republic of Macedonia

4.2 LINEAR DEFORMATIONS AND DISTORTION ISOGRAMS IN THE STEREOGRAPHIC PROJECTION OF THE REPUBLIC OF MACEDONIA

The calculation of the linear deformations is the function of the radius of the circle (the distance relative to the center of the projection). Knowing the radius of the boundary circle, it is possible to determine the maximum linear deformations in the stereographic projection of Republic of Macedonia.

The average radius of curvature at the center of the stereographic projection with a geographic latitude $\varphi_o = 41^o\ 30'\ 30''$, is:

$$R_o = 6374766.265 \text{ m}$$

and the maximum value of the linear deformations is:

$$\mu - 1 = \frac{\rho^2}{4R_0^2} 100000 = 7.18 \text{ cm/km}$$

The value of the linear deformations (7.2 cm / km) can be controlled by calculating the stereographic coordinates for the points in which the circle touches the boundary line. In this way, the following linear deformations in points 8, 14 and 17 are obtained.

Point No.	deformation (cm/km)
8	7.26
14	7.25
17	7.30

The minimum difference of approximately 1 mm/km between exactly calculated and graphically defined linear deformations is due to the limited graphic accuracy of the auxiliary map.

After the completed control, the maximum value of the linear deformations in the stereographic projection of Republic of Macedonia with the application of the tangent projection plane was determined:

7.3 cm/km

The distortion isograms in the stereographic projection are circles in the middle of the central point of the projection. They are defined with the appropriate radius values that can be obtained by transforming the formula (22):

$$\rho = 2R_0\sqrt{\frac{(\mu-1)}{100000}} \qquad (23)$$

The distortion isograms in the stereographic projection of Republic of Macedonia are presented in Table 1.

Table 1. Distortion isograms in the stereographic projection of Republic Macedonia

deformation (cm/km)	**distortion isograms (circle)**
	ρ (km)
0	0
1	40.3
2	57.0
3	69.8
4	80.6
5	90.2
6	98.8
7	106.7

The graphical representation of the distortion isograms is given in Figure 8

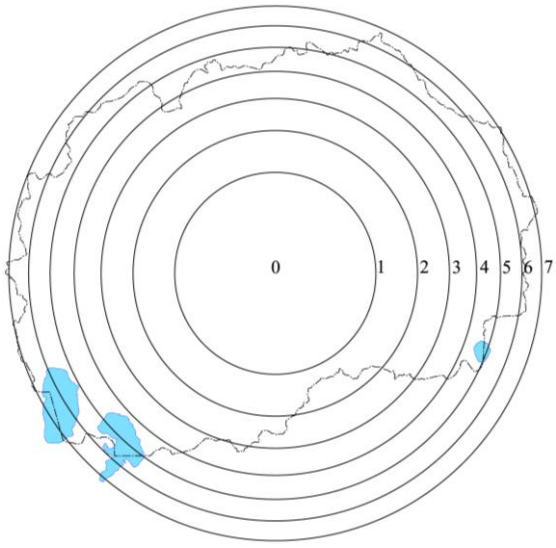

Figure 8. Distortion isograms in the stereographic projection of the Republic of Macedonia

The accuracy of the projection can be increased by introducing a negative linear deformation (-3.5 cm/km), or by introducing a secant projection plane. In this way, the maximum linear deformation is reduced (by absolute value) to half, and the deformations in the stereographic projection are distributed in the range of -**3.5 cm/km to +3.8 cm/km.**

The radius values (ρ), that define the distortion isograms after the reduction are presented in Table 2.

Table 2. Distortion isograms in the stereographic projection after the reduction

deformation (cm/km)	**distortion isograms (circle)**
	ρ (km)
-3.5	0
-3	28.5
-2	49.4
-1	63.7
0	75.4
1	85.5
2	94.6
3	102.8

The graphical representation of the distortion isograms after the reduction is given in Figure 9.

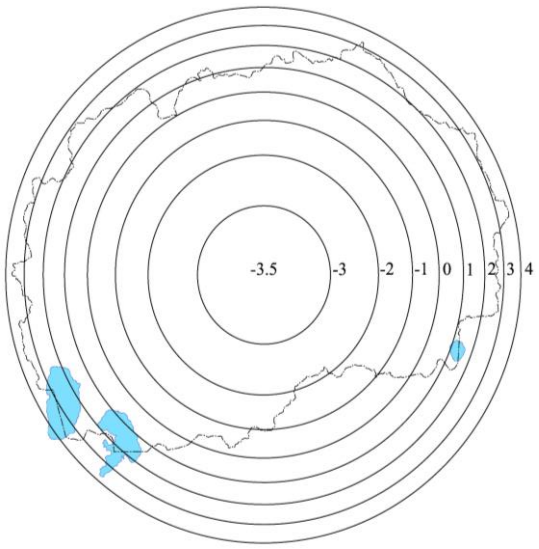

Figure 9. Distortion isograms in the stereographic projection on R. of Macedonia after the reduction

Based on the above, the basic properties of the stereographic projection for Republic of Macedonia can be sublimated:

- The maximum linear deformation, which arises from the dimensions of the boundary circle, is 7.3 cm / km in the stereographic projection of Republic of Macedonia.

- Increasing the accuracy of the projection is achieved by modulating the Cartesian coordinates with the module m = 0.999965, or introducing a negative linear deformation of -3.5 cm / km, which enables the entire territory of Republic of Macedonia to be covered with deformations that don't exceeding ±3.8 cm/km.
- The distortions of lengths are 75% smaller than the distortions in actual Gaus-Kruger projection.
- The shape of the territory of the Republic of Macedonia is very suitable for use of stereographic projection.
- The linear deformation layout is normal, and the isocols have the shape of a circle.
- There are no angle distortions.

REFERENCES

[1] Borčić B. (1955): *Matematička kartografija (kartografske projekcije)*, Tehnička knjiga, Zagreb;

[2] Jovanović V. (1983): *Matematička kartografija,* Vojnogeografski institut, Beograd.

[3] Ribarovski R., Srbinoski Z. (2008): *Scientific researches for defining of new map projection for the territory of Macedonia,* International Conference on Cartography and GIS, Borovec, Bulgaria.

[4] Србиноски З. (2001): *Прилог кон истражувањата за избор на нова државна картографска проекција*, Докторска дисертација, Градежен факултет, Скопје.

[5] Srbinoski Z (2018): Study for selecton of new state cartographic projection of the Repubilc of Macedonia, Agency for real estate cadaster, Skopje.

AUTHORS

Filip Kasapovski
MSc, Assistant
Ss. Cyril and Methodius University
Faculty of Civil Engineering – Skopje
email: kasapovski@gf.ukim.edu.mk

Slaveyko Gospodinov
PhD, Full Professor
University of Architecture, Civil Engineering and Geodesy- Sofia
email: s.gospodinov@mail.bg

Zlatko Srbinoski
PhD, Full Professor
Ss. Cyril and Methodius University
Faculty of Civil Engineering – Skopje
email: srbinoski@gf.ukim.edu.mk

Lazo Dimov
PhD, Full Professor
Ss. Cyril and Methodius University
Faculty of Civil Engineering – Skopje
Email: dimov@gf.ukim.edu.mk

Zlatko Bogdanovski
PhD, Assistant Professor
Ss. Cyril and Methodius University
Faculty of Civil Engineering – Skopje
email: bogdanovski@gf.ukim.edu.mk

Tome Gegovski
MSc,
Ss. Cyril and Methodius University
Faculty of Civil Engineering – Skopje
email: gegovski@gf.ukim.edu.mk

VERTICAL CRUSTAL MOVEMENTS IN SEISMIC ACTIVE REGIONS

This paper presents the measurements and certain vertical displacements of the Earth's crust in the seismic active area of the Skopje valley. The need for this activity was initiated by 16 earthquakes with Mw = 2.1 - 5.2 according to the EMSC that appeared in the period from 11.09 to 20.09 2016. Therefore, a precise levelling of high accuracy has been used on a part of the state levelling network from first order, which is located on the territory of the City of Skopje. In particular, height differences are determined between the benchmarks of the levelling line that pass through the blocks formed by intersection of the active faults in the area.

Key words: basic levelling network, precise levelling, geodynamics, vertical crustal movements.

1. INTRODUCTION

Since the formation of the Earth as a geological body till today, it has been constantly changing, with its individual parts being in a state of complex interactions with each other. Therefore, a modern definition of tectonic movements, as a fundamental concept of geotectonics, should be based on the assumption of the Earth as an unstable system in which the geological processes flow continuously, but unevenly with different intensity in time and space. Observations of the geodynamic processes and the determination of displacements and deformations of the Earth's crust based on geodetic measurements, is in fact examination of the time evolution of the reference system, that is, the geodetic reference networks, realized and materialized with appropriate markers on the physical surface of the Earth. [12]

Direct measurements are the basic source of information necessary to determine the character and genesis of a given geodynamic process and the phenomena associated with it. Given the nature of the methods of determining the mutual position between the points of the networks, the horizontal and vertical component of the displacements are determined by different measurements.

Therefore, in the geodetic terminology, the terms contemporary vertical movements of the Earth's crust (**CVMEC**) and contemporary horizontal movements of the Earth's crust (**CHMEC**) were imposed. [6]

The displacements are determined based on a minimum of two mutually comparable and independent measurements made over a different period of time. The differences in the positions of the points in both measurements represent the displacements in a horizontal or vertical sense, depending on the type of measurements.

In the particular case, it's a matter of precise geodetic measurements aimed at determining the vertical displacements of the Skopje valley. To this end, a precise levelling of high accuracy is applied, which is part of geometric levelling, which can provide the highest accuracy in determining height differences. The precise levelling is applied to one levelling line in the Skopje valley, where the benchmarks are located in different blocks formed by intersection of local faults: the Skopje-Kjustendil fault (which cuts the Skopje valley on the middle in east-west direction), then the Skopje-Crnogorski fault (stretching along the western slopes of the eponymous mountain) and other smaller faults.

Due to various internal and external factors over time, horizontal and/or vertical displacement of the blocks may occur, which usually last for a few seconds, known as an earthquake. The movement itself is from several millimeters to several centimeters. [7]

2. SEISMOTECTONICS, GEOLOGICAL PROCESSES AND STRUCTURES

Tectonic plates theory claims that the Earth's crust is divided into multiple plates, these plates are parts of the lithosphere that float on the subfluidic asthenosphere and move relatively one relative to another at a certain speed. [3] This constant movement of the plates is responsible for geological events such as volcanic activity, earthquakes, and the movement of continents.

The tectonic movements are manifested as deformations of the Earth's crust, these deformations are most common in the boundary zones between the plates or the blocks. These boundary zones are defined depending on the way of movement of the tectonic slabs. If two plates are moving towards one another, the collision is the boundary of convergence (***convergent zone***) these activities can cause the occurrence of earthquakes. In the case when the plates diverge, that is a boundary of separation (***divergence zone***) resulting in volcanic activities, whereas if the plates move horizontally along a vertical fault surface, that is boundary of slipping (***transformation zone***).

While tectonic plates are interacting, a lot of pressure and stress is created that exceeds the upper limit of their mechanical strength, and during that deforming, tectonic forms, known as faults, occur. [12] With the creation of the fault structure, the formed wings (blocks) in the rocks move in a horizontal or vertical or combined direction. The basic form of vertical displacements is the faults; they are usually under different slopes in relation to the horizontal. In nature, shear faults occur most often. They are further divided into: gravity or **normal faults**, **reverse faults** and peelings, sleeves and **horizontal faults**. Of course, various combinations of movements are possible, compared to the basic groups.

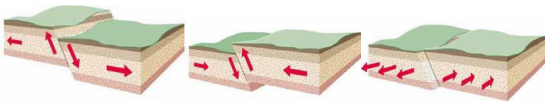

Figure 1. Normal fault (left), reverse fault (mid) and trans-current (horizontal) fault (right) [12]

2.1 TECTONICS AND NEOTECTONICS OF R. MACEDONIA

The territory of the Republic of Macedonia is located in the central part of Southeast Europe, in particular on the Balkan Peninsula. Nowadays the Balkan Peninsula lies in a collision zone between three major plates: Eurasian, African and Arabian, which are divided into smaller plates. The active tectonic processes in the eastern Mediterranean are most influenced by the following: subduction of the Adriatic micro plate under the Dinarides, subduction of the Ionian and Levant micro plains under the Hellenic trenches and the collision between the Eurasian and the Arabian plates, related to the North - Anatolian fault. [8]

From geological research, made by Dumurdjanov et al., 2005, active faults within Macedonia are summarized in Fig. 2. Three categories of faults are shown; 1) faults with evidence of active faulting, such as scarps or

offset streams (red), 2) faults with well-developed morphological expression for active faulting, but without evidence for scarps (solid blue), and 3) faults with well-developed morphological expression for the modern topography and are only suspected to be active (dashed blue). [4]

In engineering, special attention is paid to the existence of so-called **active faults**.

They are structures where displacements occur and in modern days through their length there is release of seismic energy in the form of earthquakes.

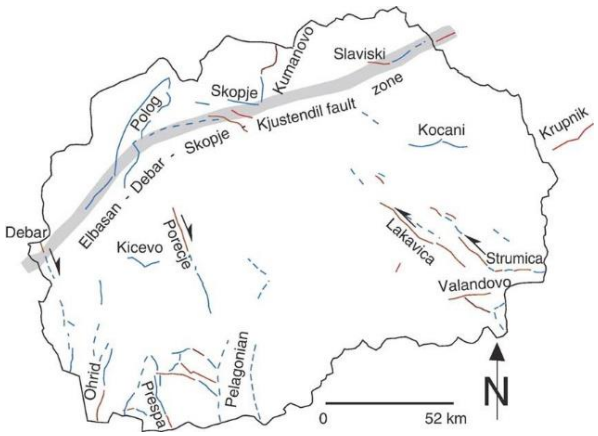

Figure 2. Active faults in Macedonia [4]

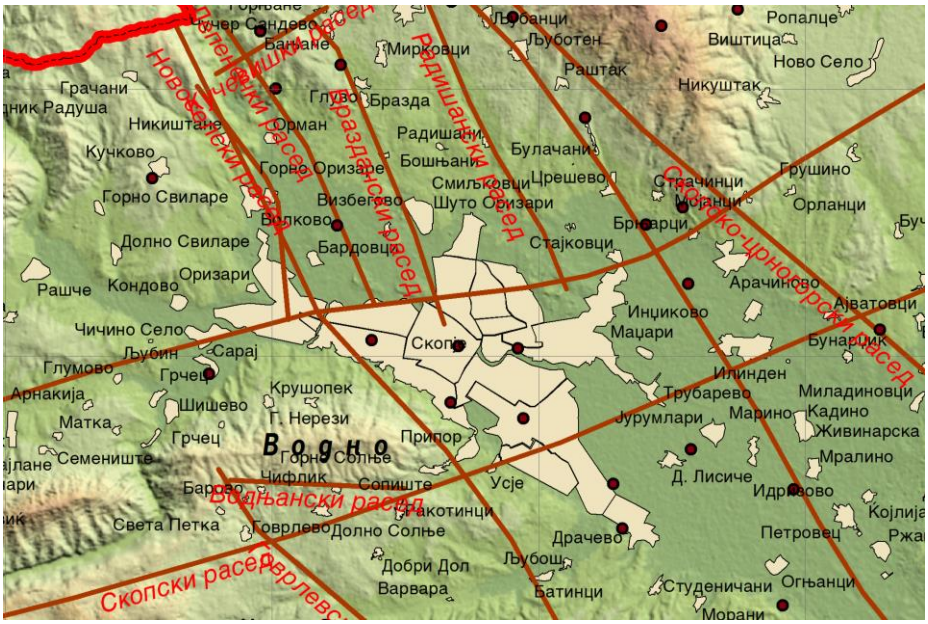

Figure 3. Neotectonic faults in the Skopje valley [3]

When it comes to active faults, that is, reactivated pre-neotectonic faults, it should be emphasized the fault that is considered to have the most significant role for the appearance of most of the earthquakes in the territory of the Skopje valley. It is about the Skopje fault, which represents a connection between the Debar-Kriva Palanka transversal dislocation in Macedonia. This dislocation starts from the city of Elbasan in the Republic of Albania through Debar, Mavrovo, Skopje, Kriva Palanka and Kyustendil in the Republic of Bulgaria. [3]

Neotectonic longitudinal faults are a special characteristic of the Skopje valley. They are concentrated in two areas, and are limited by the Skopje dislocation, that is, the Skopje fault. The division was made in the northern and southern regions defined in relation to the Skopje fault. In the northern region that have a direct impact on the Skopje valley, there are five fault structures: Radishanski, Brazdanski, Lepenicki, Novoselski and Svilarski fault. [3] Most of the above-mentioned faults cross into nodes with the most expressed potential lability (instability).

2.2 SEISMIC ACTIVITY ON THE TERRITORY OF R. MACEDONIA

The Skopje valley has large seismicity, like the majority on the territory of the Republic of Macedonia, which belongs to the central active seismic part of the Balkan Peninsula. In this region, there is often occurrence of catastrophic earthquakes, which reached epicentre intensity to X MSK-64 and magnitude to 7.8 degrees (which is the highest observed magnitude on the Balkan Peninsula),

is the Pehchevo-Kresna earthquake of April 4, 1904, with a magnitude from 7.8 degrees on Richter scale.

The Vardar seismogenic zone is one of the weakest tectonic units with particularly expressed seismicity in the areas of crossing of reactivated old faults in a Vardar direction with neotectonic faults that predominantly stretch in a transverse direction.

The **Skopje epicenter area** - related to the contemporary tectonic activity of the Skopje depression, which represent a neotectonic depression. According to the morphological characteristics it is divided into three segments: a modern Skopje field, areas built of neogene sediments and surrounding mountain terrains.[8]

When it comes to instrumental data on earthquakes in this area, it should be noted that such data exist since 1900. According to these data, two earthquakes were registered on the territory of the Skopje epicentre region, followed with human casualties and material damage. One of them happened on 10.08.1921, on the northern slopes of the mountain range Skopska Crna Gora with a magnitude M_L = 6.2 degrees on the Richter scale and with a depth of 20km. The second earthquake is the famous Skopje earthquake of July 26, 1963, with a magnitude of M_L = 6.1 degrees on the Richter scale and with a depth of 5km of the hypocentre in which a large number of human lives were lost and created great material damage.

For our research, very important is probably the centennial seismic cycle that struck Skopje and

its surroundings in 2016 from 11 to 14 September, which was located 3.5-7.0 km east from the seismic hotspot from 1963. In the cycle, a total of 16 earthquakes occurred with M_w = 2.1 - 5.2. The first strong earthquake occurred on 11 September at 6 am and 58 minutes, the hotspot is about 10 km northeast of the centre of Skopje, between the village of Arachinovo and the village of Creshevo, with a depth of about 5 km, a magnitude of 4.1 degrees, and the intensity around the V- VI degrees by EMS (European macroseismic scale, also known as EMS-98). The second strong earthquake occurred again on **September 11 at 3 pm and 10 minutes**, with a stronger intensity of **5.2 -5.3** degrees or about 15 times the energy of the first quake. The hotspot of this earthquake was several kilometres east of the centre of Skopje, at a depth of about 10 km. This earthquake is the strongest in the group of earthquakes. The last earthquake occurred on September 14 at 1 pm and 32 minutes, with a magnitude of 3.1 degrees and a depth of 3 km. Such strong earthquakes in the Skopje region, according to data from the seismological observatory at PMF in Skopje, appear on average once every 100 years. It is believed that the strongest expected or occurring earthquake in the Skopje's seismic region can reach magnitude to 6.5 degrees, something slightly stronger than that of the great earthquake in 1963 (6.1 degrees). The probability of an earthquake with magnitude greater than 6 degrees is once in 500 years. [7]

Date	Time UTC	Latitude	Longitude	Depth	Magnitude Type	Magnitude
11.09.2016	04:58:01	42	21.51	4	mb	4.2
11.09.2016	05:00:05	41.99	21.49	3	ML	2.8
11.09.2016	13:10:07	41.98	21.5	4	mb	5.2

Table 1. Official data from EMSC (European Mediterranean Seismological Centre) [7]

The earthquakes of September 11-14 occurred just beside the faults juncture, where the Skopje-Kustendil and the Skopje-Crnogorski fault intersect, at a depth of about 5-10 km and in a diameter of about 5 km along the fault structures. Along the two faults, the Skopska Crna Gora block is moving vertically and in the west direction, as evidenced is the turning of the valleys of rivers descending from the mountain. [7]

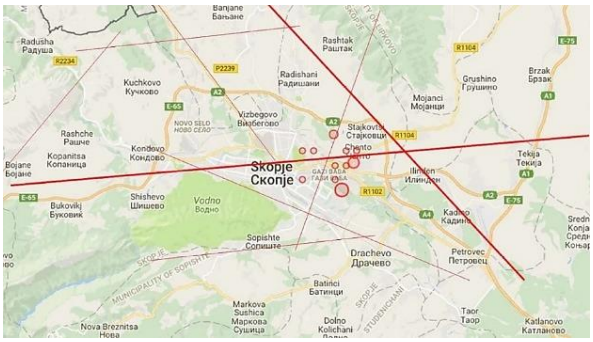

Figure 4. Epicentres of the earthquakes from 11 to 14 September 2016 stronger than 2.5 M (circles) and the main fault cracks [7]

3. THE NEW LEVELLING NETWORK OF THE R.MACEDONIA

The basic levelling network is a part of geodetic networks, which serves as the altimetric base for preforming of all height surveys in the Republic of Macedonia, as well as for realization of important scientific engineering and technical tasks. It is divided into several ranks, of which **I** and **II** rank, are of the highest accuracy and used for scientific research in determining the figure of the Earth and the vertical movements of the Earth's crust, as well as the differences in the levels of seas and oceans.

The new levelling network with high accuracy (NVT3) is consisting of 1098 levelling points (benchmarks) connected with 49 levelling lines and 19 polygons, plus 12 lines for connection with neighbouring countries. The total length of levelling traverses is 2189 km, with an average distance of 1800 m between benchmarks and average perimeter of the polygons with 166 km. It is consisting 28 fundamental benchmarks and 31 nodal points. [9]

Figure 5. Fundamental Benchmark Skopje

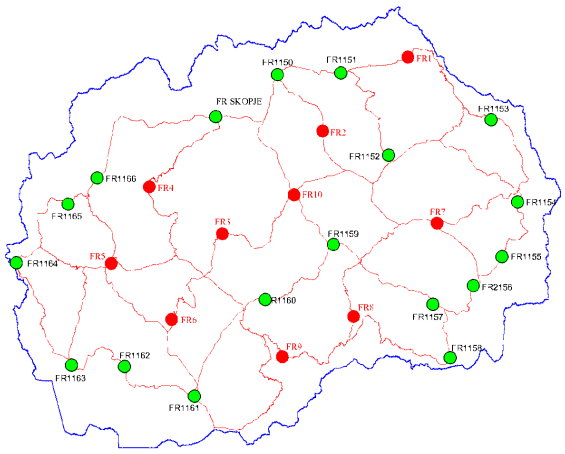

Figure 6. Location of the fundamental benchmarks of the new levelling network

3.1 GRAVIMETRIC NETWORK

Gravimetric measurements were carried out on the entire territory of the Republic of Macedonia for the purpose of defining different physical height systems.

Rank	Zero	First	Second
Year of measure-ment	2010	2013	2014
Number of points	3	25	2310
Accuracy	3 μGal	13 μGal	< 60 μGal

Table 2. Basic data for the gravimetric network of RM

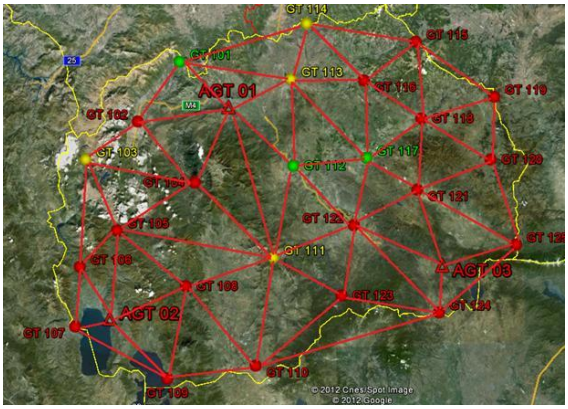

Figure 7. Gravimetric network of the first order

4. PRACTICAL MEASUREMENTS

First, an analysis of the location of the faults in the Skopje valley was made and their expansion in relation to the levelling traverses from the state levelling network of the first rank, in order to get an idea of which levelling traverses have benchmarks that are located on different blocks formed from the intersections along the fault structures.

Parts from the levelling traverses V2 and L17 are selected, from which is formed levelling traverse with total length of 9.2km, which consists of five levelling sides.

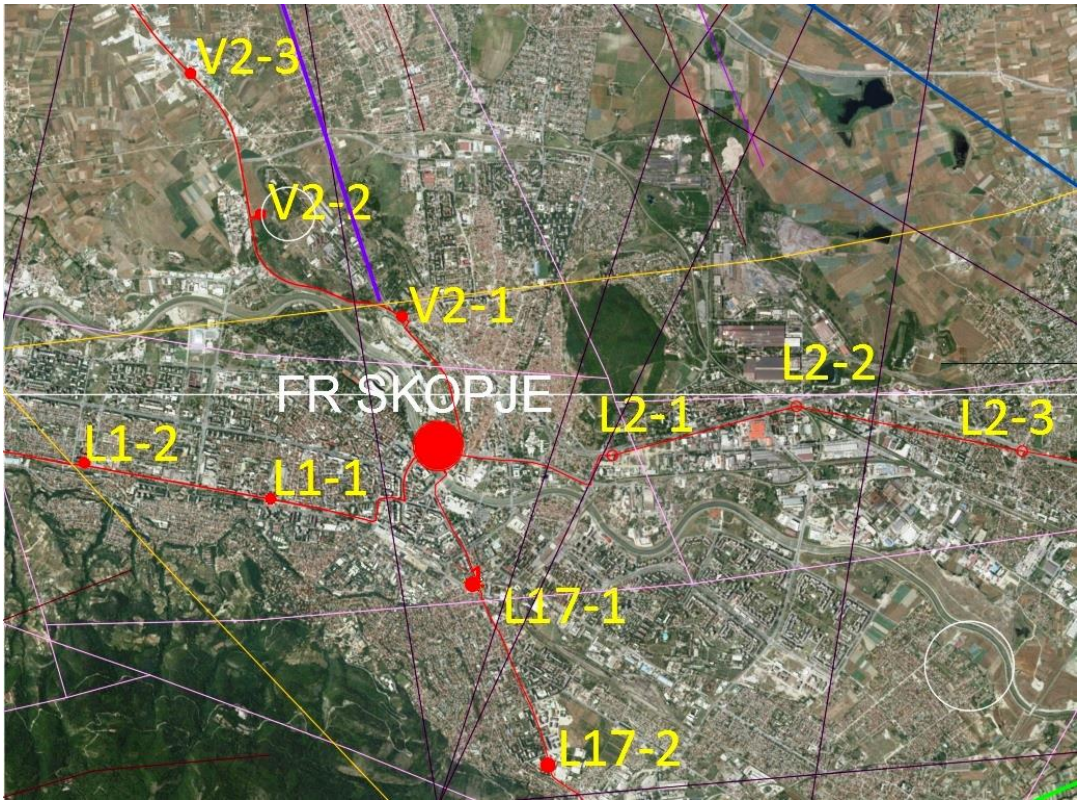

Figure 8. The location of the faults in the Skopje valley and their expansion in relation to the levelling traverses from the state levelling network of the first order

Field activities were carried out in the period from 16 to 20 July 2018. While planning the measurement schedule and after the organized field inspection, it was ascertained that the R_2 benchmark from the levelling line V2 was destroyed, in order to meet the criterion for distance between two successive first-order benchmarks, a new auxiliary benchmark Rp_2 was placed near the old benchmark R_2.

4.1 GEOGRAPHICAL AND GEOLOGICAL DESCRIPTION OF THE LEVELLING ROUTES

The V2 line extends geographically in the north-west direction, from the Skopje exit passes through the industrial zone of Vizbegovo, goes along the national road which is in good condition, but not very wide for the frequency of the traffic that passes through it.

From the beginning of the route, until the connection to the main road for the Blace border crossing, the terrain from geological aspect is built of Miocene sediments, composed of jackals, sands, marls and clays.[1]

The line L17 starts from the fundamental FR-SK benchmark under the fortress in Skopje, near the Goce Delchev Bridge, geographically extends in the north-west direction along the regional road Skopje-Sopiste. The route of the line L17 from the starting point crosses the river Vardar to the square "Macedonia" then, passing through the main access roads continues through the city Skopje to the exit from Skopje near Kisela Voda at the foothills of Vodno.

The whole terrain through which the route of the levelling line crosses is built from quaternary sediments represented as lower river terraces and alluvial sediments formed around the river Vardar. These sediments are products of the youngest erosion processes, which last even today. They are composed of various granulated, unsorted gravel, sands and clays, which originate from the rocks of the watershed of the river Vardar and its tributaries in the Skopje valley. [1]

4.2 MEASUREMENT OF HEIGHT DIFFERENCES

Measurement of height differences was made in accordance with the recommendations of the technical specification with appropriate instruments, equipment and observation procedures, the required accuracy was fully met. The precise digital level used is **Leica**

DNA 03, equipped with two three metre barcoded levelling rods with invar tape, with original holders and metal slippers. The instrument has a declared accuracy of **0.3 mm/km.** During the measurement, readings and registration of the temperature values were performed. At a certain time interval of 2 hours on three different places, the lower, middle and upper part of the Invar rods with the help of an appropriate instrument.

Figure 9. Measuring the temperature of the Invar rod

Conditions that are met while measuring the height differences:

- Before starting the measurements, the instrument and the invar rods are acclimatized to external conditions for half an hour;
- The values of the angle "*i*" are determined. The values for the angle "*i*" are not included in the instrument in the form of corrections in the measurement of the height differences, but they are recorded in separate files. The absolute value of the angle "*i*" does not exceed 15 ";
- Double measurements were made by changing the height of the instrument;
- The measurements of each station are made from the middle where the difference between the front and rear sight distance is not greater than 3m, also attention is paid on the change of the position of the tripod legs when changing the stations;
- The number of stations in the precise levelling of the height difference between two benchmarks is even;
- The wind speed did not exceed 3 m / s, and when sighting the conditions of the front and rear invar rods were approximately the same;
- The length of the sight does not exceed 30m, while the height of the sight reading is not less than 0.5m or greater than 2.5m.

The results of the measurements of the height differences on the levelling sides are shown in the levelling field book, and from the field book a table is prepared containing the data for the mean values of the height differences of the levelling sides and the deviations from the front and back levelling.

Nº BM	lm between BM, S, km	Height difference, m		d=II - I mm	Average value of height differences
		I	II		
FRSK V2-R1	2.01	28.53262	-28.53317	-0.55	28.53290
V2-R1 V2-R2p	2.18	20.9649	-20.96575	-0.85	20.96533
V2-R2p V2-R3	1.36	-14.1584	14.15921	0.84	-14.15879
FRSK L17-R1	1.65	-4.51362	4.51348	-0.14	-4.51355
L17-R1 L17-R2	1.95	-2.69487	2.69573	0.86	-2.69530

Table 3. Measured height differences

From the data in the field books, the following basic characteristics of the measurements can be noted:

- Minimum distance instrument-invar rod occurs in the level-side V2-FR-V2-R1 and is 5.85 meters;
- The maximum distance of the instrument-invar rod occurs in the level-side V2-FR-V2-R1 and is 29.77 meters;
- The minimum number of levelling stations occurs on the level-side V2-R3-V2-R2p and is 28;
- The maximum number of levelling stations occurs on the level-side V2-FR-V2-R1 and is 54;

4.3 QUALITY CONTROL OF THE MEASUREMENTS

Levelling results are checked before further processing:

- By calculating the values for the height differences measured back and forth;
- By creating differences from the height differences between the front and back levelling;
- By comparing with the criteria defined for the realization of the measurements.

The basic criteria of the accuracy for performing the measurements are defined through:

Allowed deviation of the dual height difference (forward-backward):

$$\Delta_{\Delta H}(mm) = 2\sqrt{s} \qquad (1)$$

s - length of the levelling line in km.

Allowed deviation of closing of the polygons:

$$\Delta_{P}(mm) = 4\sqrt{s} \qquad (2)$$

s - length of closed polygon in km.

From the analysis of the difference between the height differences in the levelling sides (forward-back) and the allowed deviations, it can be noted that all the height differences fulfil the condition of accuracy.

4.4 DETERMINATION OF VERTICAL MOVEMENTS

Vertical shifts in the Earth's crust are determined by comparing measured height differences from the current epoch 2018 and the initial measurements after the establishment of the new levelling network from first order, realized in 2013.

From	To	Distance [m]	Dh-2013	Dh-2018	Dh [m]
FRSK	**V2-R1**	2014.37	28.53066	28.53290	**-0.00223**
V2-R1	**V2-R3**	3545.00	6.807685	6.806535	**0.00115**
FRSK	**L17-R1**	1654.71	4.512605	4.51355	**-0.00095**
L17-R1	**L17-R2**	1951.91	2.690815	2.69530	**-0.00449**

Table 4. Display of the vertical shifts

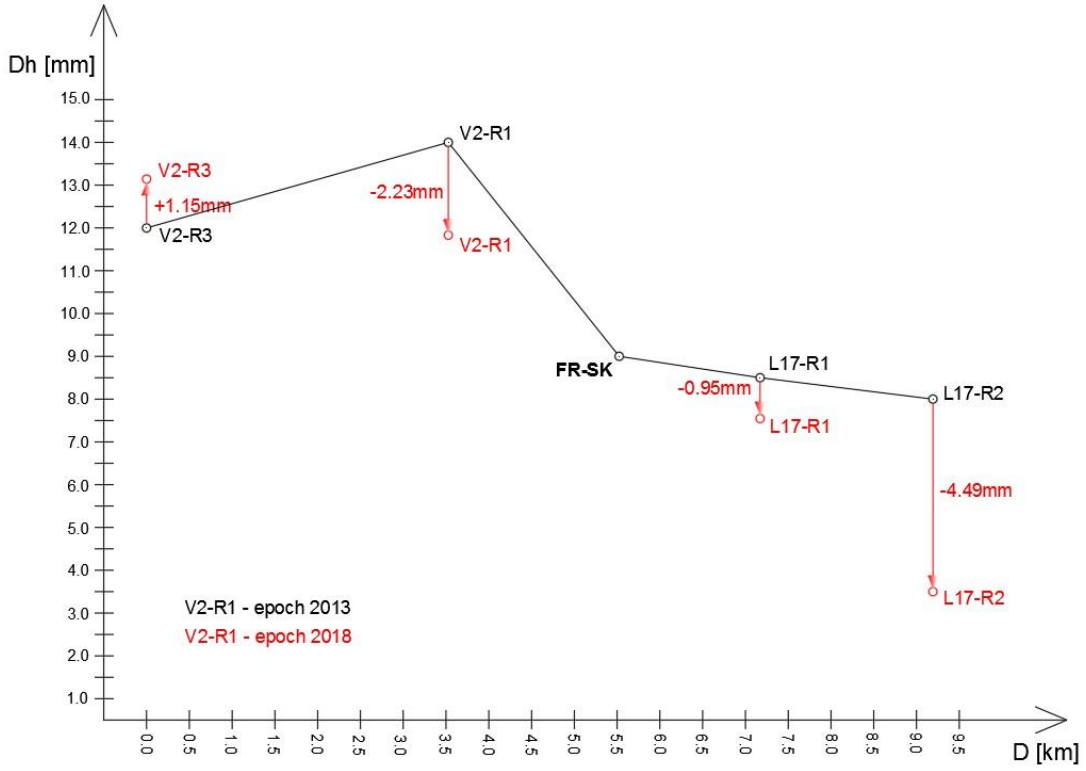

Figure 10. Graphic display of vertical displacements

5. CONCLUSIONS

Due to the movement of the lithospheric plates, the geodetic coordinates of the points on the surface area of the plates change their values over time, which makes them dependent on the epoch in which the observations were made. Geometric levelling is the oldest and only geodetic method that, with the accuracy it provides, meets the high accuracy criteria for determining the vertical component for exploration of seismic and tectonic processes.

When interpreting the results for the purposes of geodynamics, it should be borne in mind that the obtained data refer to the differences

between uncorrected directly measured height differences between the benchmarks in both epochs. In order to obtain the definite heights of the benchmarks, it is necessary to realize and process two types of measurements, the basic precise levelling measurements, and additionally perform gravimetric and GNSS measurements of the benchmarks of the levelling network, as well as measurements and registration of temperature, humidity and pressure.

The data processing itself includes:

- First of all, the quality control of the measurements which was made in this paper and it was concluded that all levelling measurements were performed in accordance with the defined criteria for control and monitoring of the measurements, namely: stations, levelling sides and levelling traverses from the network;
- Next, the results of the levelling measurements should be corrected with geometric corrections;
- To perform a transformation of directly measured height differences in different physically defined height systems;
- Adjustment of the levelling network of high accuracy;
- And in the end conducting statistical tests and assessment of accuracy.

Figure 11. Level station at the Stone Bridge Skopje

6. REFERENCES

[1] Agency for Real Estate Cadastre (2012), Reports for reconnaissance of polygons of the new levelling network, Skopje.

[2] Agency for Real Estate Cadastre (2013), Reports for height differences measurement of levelling lines of the new levelling network, Skopje.

[3] Bogdanovski Z., (2015), Определување на геодинамиката на Скопската котлина врз основа на геодетски мерења, Phd thesis, Faculty of Civil Engineering, UKIM in Skopje.

[4] B. Clark Burchfiel et al., (2006), GPS results for Macedonia and its importance for the tectonics of the Southern Balkan extensional regime, *Tectonophysics*.

[5] Dumurdjanov N. et al., (2016) Seismotectonic zones and seismic hazard in the Republic of Macedonia.

[6] Gospodinov S. (2011), Определеяне на блоково обусловени равнини деформации на Земната кора посредством измерени пространствени хорди, *Военo-географска служба*.

[7] Milevski I. (2016): For the Skopje earthquake of September 11, 2016. Published online on IGEO Portal http://www.igeografija.mk/Portal/?p=6876 (in Macedonian; accessed on 15.10.2018)

[8] Mirceski D. (2018), Application of block conditioned flat deformations in the analysis of geodynamic events, Master thesis.

[9] Odalovic O. (2009), *Study for the levelling and gravimetric network in R. of Macedonia*, Agency for Real Estate Cadastre, Skopje.

[10] Srbinoski Z. (2008), *Physical Geodesy*, Faculty of Civil Engineering, Skopje.

[11] Srbinoski Z., et al., (2017),Geodetic projects as part of main project for new basic levelling network, *SJCE, Vol. 6 Issue 2*, Skopje.

[12] Sušić Z. et. al., (2016), Application of geometric analysis of deformation measurement in monitoring of geodynamic process, *Conference paper.*

SJCE

SCIENTIFIC JOURNAL OF CIVIL ENGINEERING

SS CYRIL AND METHODIUS UNIVERSITY
FACULTY OF CIVIL ENGINEERING